ELSEVIER

Chemical Geology 239 (2007) 284–304

CHEMICAL GEOLOGY
INCLUDING
ISOTOPE GEOSCIENCE

www.elsevier.com/locate/chemgeo

Cycling of B, Li, and LILE (K, Cs, Rb, Ba, Sr) into subduction zones: SIMS evidence from micas in high-*P*/*T* metasedimentary rocks

Gray E. Bebout [a,*], Ann E. Bebout [b], Colin M. Graham [c]

[a] *Department of Earth and Environmental Sciences, 31 Williams Drive, Lehigh University, Bethlehem, Pennsylvania 18015, USA*
[b] *Department of Physical Sciences, Kutztown University, Kutztown, Pennsylvania 19530, USA*
[c] *School of GeoSciences, University of Edinburgh, Edinburgh EH9 3JW, UK*

Accepted 23 October 2006

Editor: S.L. Goldstein

Abstract

The Catalina Schist (California) affords a unique opportunity to evaluate the effects of varying prograde *P*–*T* paths on the magnitudes of devolatilization and chemical/isotopic alteration of subducting sediments. Analysis of a suite of trace elements (Li, B, Rb, Sr, Cs, Ba) in micas obtained by secondary ion mass spectrometry (SIMS) complements previously published whole-rock data for metasedimentary rocks in the Catalina Schist and circumvents problems associated with chemical/isotopic overprinting during retrogression, further elucidating trace element redistribution during devolatilization along prograde *P*–*T* paths.

SIMS mineral analyses confirm the inference from the whole-rock data that white mica (and in a few higher-grade samples, also biotite) is the dominant reservoir for B, Rb, Ba, and Cs. The mineral residency of Li and Sr is more complex, as Li is also highly concentrated in chlorite (where present) and in some amphiboles, and Sr whole-rock budgets are strongly influenced by the presence or absence of Ca-rich phases (e.g., lawsonite, clinozoisite, minor carbonate and titanite). Changes of concentrations of B and Cs, in white micas, with increasing metamorphic grade parallel the whole-rock trends, further demonstrating the loss of these elements from recrystallizing white micas during prograde devolatilization reactions. Trace element data for other minerals in the metasedimentary samples (Ca–Al silicates, plagioclase, chlorite, biotite, garnet, kyanite) confirm expected concentrations as related to ionic radius and charge and demonstrate element redistribution during prograde (and retrograde) reactions. For amphibolite-facies metasedimentary rocks, multiple generations of white mica, including a finer-grained, higher-Si generation related to retrogradation, have distinct trace element compositions. In pegmatites produced by partial melting at amphibolite-facies conditions, B, Li, and the LILE are similarly concentrated in coarse-grained muscovite, indicating inheritance of trace element compositions from their metasedimentary sources.

These SIMS data, combined with the whole-rock data for the same samples, demonstrate that the deep transfer of relatively "fluid-mobile" trace elements is strongly dependent upon the prograde *P*–*T* path experienced by the subducting sediments. Efficient retention of B, Cs, and N in micas, to depths of >40 km, is evident from study of these and other forearc metasedimentary suites that experienced low-*T* prograde paths representative of most modern subduction zones, and is consistent with models invoking additions of these elements from the slab into arc source regions, perhaps to contribute to the across-arc chemical trends (Be/Be, B/La, Cs/Th, Ba/Th) observed in some margins.

Keywords: Devolatilization; Subduction zones; Chemical cycling; Blueschist; White mica; Ion microprobe

* Corresponding author.
E-mail address: geb0@lehigh.edu (G.E. Bebout).

0009-2541/$ - see front matter © 2006 Elsevier B.V. All rights reserved.
doi:10.1016/j.chemgeo.2006.10.016

1. Introduction

Studies of uplifted tracts of high-*P*/*T* metamorphic rocks (e.g., blueschist- and eclogite-facies suites, representing subduction to depths of ~5 to >100 km) can provide detailed information regarding the extent of loss of volatile components during prograde metamorphism along relatively cool *P*–*T* paths characteristic of modern subduction zones (see Bebout, in press). Work on the Catalina Schist, Franciscan Complex, and Western Baja Terrane paleoaccretionary suites indicated that, in cool subduction zones, much of the sedimentary LILE, organic C–N, and B–Li inventory can be retained to depths of up to 51 km (Bebout and Fogel, 1992; Bebout et al., 1993, 1999; Sadofsky and Bebout, 2003). Work by Busigny et al. (2003) on mica K, Rb, Cs, H, and N contents and C–H–N isotope compositions in Schistes Lustrés and Lago di Cignana metasedimentary rocks (Italian Alps; with peak P corresponding to ~60–90 km depths) provides an indication of possible deeper retention of these elements (also see Bebout et al., 2003, 2004). Recent studies have stressed the significance of micas as the primary mineral host dictating recycling behavior of a number of trace elements used as tracers of slab additions in arc lavas (B, LILE such as Rb, Ba, and Cs; Domanik et al., 1993; Bebout et al., 1993; Sorensen et al., 1997; Bebout et al., 1999; Zack et al., 2001, 2002; Catlos and Sorensen, 2003; Busigny et al., 2003; experimental work by Domanik and Holloway, 1996). Zoisite–clinozoisite and lawsonite are thought to exert important controls on budgets of REE (particularly the LREE) and Sr during prograde subduction (for discussion of clinozoisite, see Brunsmann et al., 2000, 2001; for discussion of lawsonite, see Domanik et al., 1993; Pawley and Holloway, 1993; Pawley, 1994; King et al., 2004; Usui et al., 2006).

The Catalina Schist (California), which records high-*P*/*T* metamorphism during Cretaceous subduction, contains metasedimentary rocks (greywackes and shales) and metamafic rocks (basalts and gabbros) ranging in grade from lawsonite–albite to amphibolite facies (peak conditions of ~275 to 750 °C, 5 to 12 kbar; Bebout and Barton, 1993; Grove and Bebout, 1995). In the Catalina Schist, the preservation of tectonometamorphic units representing metamorphism at 15–40 km depths in a subduction setting (see discussions of tectonic model by Grove and Bebout, 1995) allows evaluation of the magnitude of forearc devolatilization as a function of prograde *P*–*T* history (see Bebout et al., 1999; Fig. 1). In this paper, we present single-mineral major and trace element analyses, obtained by SIMS (spatial resolution of ~15 μm) and electron microprobe

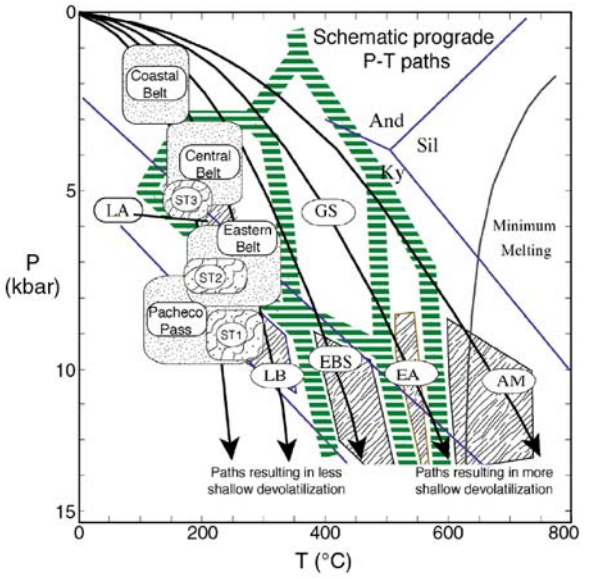

Fig. 1. Pressure–temperature diagram showing estimates of peak metamorphism for paleoaccretionary prism rocks from California, USA, and Mexico (see Grove and Bebout, 1995, for details regarding the generalized phase equilibria and stability fields compiled on this diagram). Arrows are schematic prograde *P*–*T* paths rocks might take in subduction zones, reflecting a wide range in thermal structure. LA = lawsonite–albite, LBS = lawsonite–blueschist, EBS = epidote–blueschist, GS = greenschist, EA = epidote–amphibolite, and AM = amphibolite. Various units of the Coast Ranges Franciscan Complex are indicated ("Coastal Belt", "Central Belt", and "Eastern Belt", in order of increasing peak metamorphic pressures thus depths of underthrusting; see Sadofsky and Bebout, 2003, 2004; Blake et al., 1987). Also indicated is the peak *P*–*T* for the Franciscan Complex metagreywackes at Pacheco Pass, California (estimates from Ernst, 1993). Fields labeled "ST1", "ST2", and "ST3" indicate peak conditions for tectonometamorphic units of the Western Baja Terrane (from Sedlock, 1988).

methods, for metasedimentary rocks of the Catalina Schist, and integrate these data with previously presented whole-rock major and trace element data for the same rocks (see A.E. Bebout et al., 1995; G.E. Bebout et al., 1993, 1999). Compositional trends in the whole-rock and mineral analyses may be linked with metamorphic reaction histories and the mineral hosts for trace element inventories identified to further elucidate chemical evolution during prograde and exhumation-related histories of the rocks. We examine the trace element redistribution during devolatilization of the Catalina Schist metasedimentary rocks as a function of metamorphism along differing prograde *P*–*T* paths, and compare our findings with data and models for devolatilization recently presented by others (e.g., Zack et al., 2001; Melzer and Wünder, 2001a,b; Busigny et al., 2003). We show that white micas dominate the whole-rock budgets of a number of trace elements recently used to

trace slab + sediment-derived aqueous "fluid" components in arc lavas (particularly B, Rb, Cs, and Ba).

2. Analytical techniques

In situ analyses for Li, B, Rb, Sr, Zr, Cs, Ba, Y, and Ce in amphibole, chlorite, biotite, white mica, clinozoisite, lawsonite, garnet, and plagioclase were obtained using the Cameca ims-4f ion microprobe at the University of Edinburgh (for detailed description of analytical conditions, uncertainties, and data reduction, see Moran, 1993). Polished thin-sections were coated with gold (200–300 Å) and sputtered with a primary negative $^{16}O^-$ beam (~15 μm in diameter, 8 nA current, 15 KeV net impact energy). Positive secondary ions of Li, B, Rb, Sr, Zr, Cs, Ba, Y, and Ce were accelerated (4500 eV) into the mass spectrometer, separated (mass resolution ~300), energy filtered (to significantly reduce molecular species), and counted using a Balzers electron multiplier. Counts (counts per second, CPS) were corrected for dead time, background matrix effects and minor remaining interferences, where necessary (see Table 1 below). Ion intensities of each element were calculated relative to Si, and concentrations were calculated from the raw data assuming that the relative ion yield for the element in the standard (SRM610 standard glass; see Hinton, 1990, 1999) equals the relative ion yield for the element in the unknown, i.e.

$$\frac{(\mathrm{CPS}/\mathrm{conc})\mathrm{el}}{(\mathrm{CPS}/\mathrm{conc})\mathrm{Si\ SRM610}} = \frac{(\mathrm{CPS}/\mathrm{conc})\mathrm{el}}{(\mathrm{CPS}/\mathrm{conc})\mathrm{Si\ unknown}}.$$

This assumption is an approximation. In their measurements of Li, Be and B in the Allende meteorite, Phinney et al. (1979) estimated that matrix effects were <50% of the measured concentration for spinel and melilite based on analyses of several tourmaline standards. Similarly, Kovalenko et al. (1988) obtained ion yields within a factor of two for crystals and SRM610 glass for Li, Na, K, Rb and Sr. Ion yields for Cs, Ba, La and Ce in two glasses also agreed to within a factor of two. Jones and Smith (1984) found that the ion yield of B from standard micas was equal to the ion yield in silicate glass. Hervig (1985) reported agreement within 5% for count rates for B in crystalline and glassy reedmergnerite ($NaBSi_3O_8$). Although the ion-probe measurements are standardless at present (and there is no physical model to predict the relationship between concentration and intensity of the various ions), the relative differences in concentration between analyses in the same phase should be correct. Shimizu et al. (1978) estimate the precision of ion-intensity ratio measurements (trace element/silicon) at generally better than 5–10% in garnet and clinopyroxene.

Errors based on counting statistics vary with the number of counts, and thus with the sensitivity of the element. For example, approximate counting errors in percent are (at the 1 and 500 ppm levels, respectively): Li (1 and 0.1); Ce, B, Sr, Y, Ba, Rb and Zr (2–4 and 0.2–0.3); Cs (5–7 and 0.4).

Chemical compositions of micas and other minerals were determined with the automated Cameca "CAMEBAX-microbeam" electron microprobe at the University of California, Los Angeles (UCLA), using oxide and silicate mineral standards, a ZAF-correction procedure, and a beam current of 13 nA at 15 kV. Where grain sizes permitted, a slightly defocussed beam (~5–10 μm diameter) was used for feldspar and mica analyses to avoid devolatilization of alkali elements during analysis.

3. Results

Fig. 2 summarizes the mineralogy and mineral chemistry of metasedimentary rocks in the Catalina

Table 1
Ion microprobe trace element analysis parameters

Isotope measured	Abundance correction	Sensitivity (cps/ppm/nA)	Interferences	Other
^{7}Li	Yes	20		Sample contamination; count rate at beginning of analysis not used reference element
^{11}B	Yes	5		
^{30}Si	Yes			
^{85}Rb	Yes	1	$^{57}Fe^{28}Si$, $^{56}Fe^{29}Si$	Interference correction based on $^{28}Si^{56}Fe$ measured at mass 84 after correction for ^{84}Sr
^{88}Sr	Yes	3		
^{89}Y		4		
^{90}Zr	Yes	2	$^{89}Y^{1}H$	Interference correction applied if Y is high
^{133}Cs		0.5		
^{138}Ba	Yes	1.3	^{138}Ce	Interference correction based on ^{140}Ce
^{140}Ce	Yes	1.3		

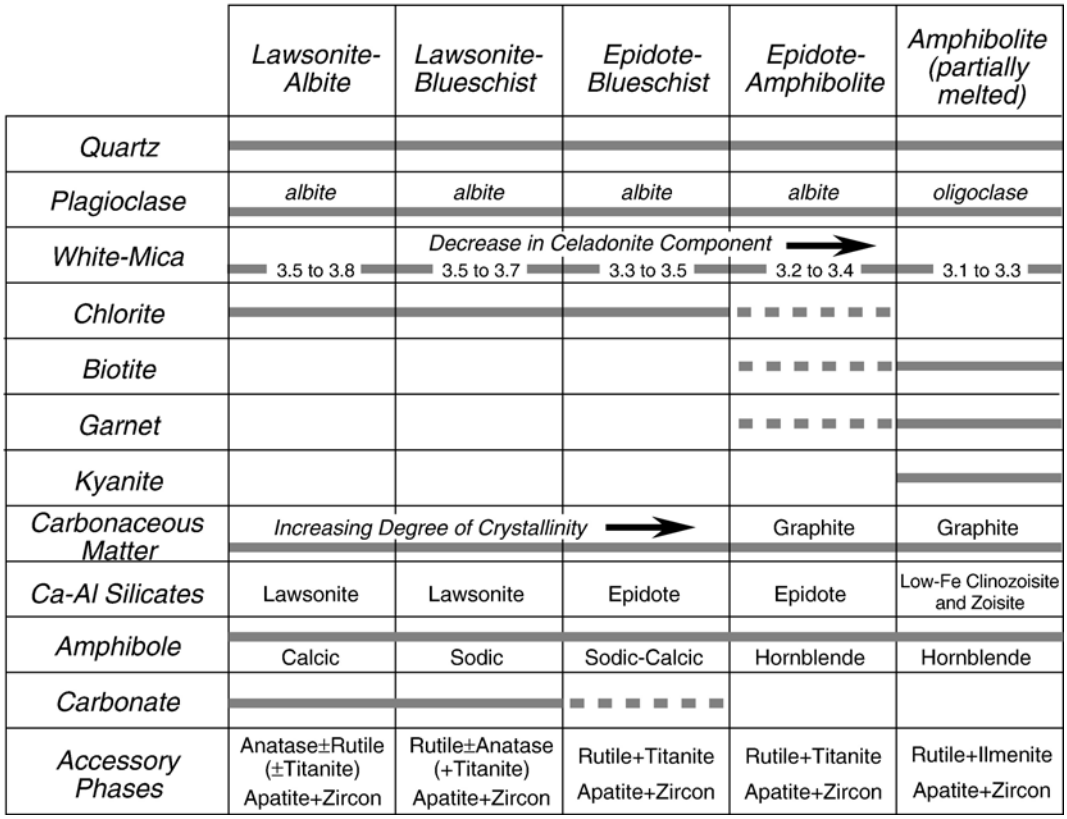

Fig. 2. Mineral assemblages, mineral chemistry, and textures in metasedimentary rocks of varying metamorphic grades in the Catalina Schist. Mineral assemblage information from Grove and Bebout (1995), Sorensen (1984), and Altheim (1997). For white micas, total Si atoms per formula unit (calculated based on 11 oxygens) are given (see Grove and Bebout, 1995). Carbonaceous matter in low-grade rocks (at grades of less than epidote–blueschist) is poorly crystalline material, whereas in the higher-grade rocks, it is more graphitic in structure (Altheim, 1997). The carbonaceous matter shows shift in $\delta^{13}C$ which correlates with N-isotope shifts and the trends in trace element compositions in this paper (see Bebout, 1995).

Schist. At each grade, rocks show large variations in the modal proportions of these minerals (reflected in varying major element whole-rock contents; see data in Bebout et al., 1999). Representative ion microprobe data, normalized to total Si content for individual mineral spots obtained by electron microprobe techniques, are provided in Tables 2 and 3 (the full dataset is available from the authors upon request), as are electron microprobe major element analyses for the white-mica spots. In Fig. 3, the concentrations of the elements on which this paper focuses (i.e., excluding Zr, Ce, and Y) are plotted as functions of mineralogy and sample/metamorphic grade, demonstrating the principal hosts for each of the trace elements (B, Li, Cs, Ba, Rb, Sr).

3.1. Boron

Phengite is the dominant mineral host for B, with white micas in all samples having higher concentrations than whole-rocks (see Fig. 3A), even in samples containing tourmaline (because of the much greater modal abundance of the micas; see Moran, 1993). Minor tourmaline (one or two small grains per thin section) has been identified in only 5 of the 42 samples analyzed for whole-rock compositions by Bebout et al. (1999; samples 7-2-132, 6-3-2I, 328-4A, 6-3-53, and 7-3-43), and we obtained ion microprobe analyses for all five of these samples. Tourmaline is abundant only in sample 6-3-53 (see B isotope analyses of tourmaline in this sample in Bebout and Nakamura, 2003). In the lower-grade units (lawsonite–albite and lawsonite–blueschist grades), grain sizes make it difficult to obtain SIMS analyses (with ~15 μm spatial resolution) for individual white-mica grains and, in some cases, white micas are clearly intergrown with chlorite at fine scales (also see SIMS data for chlorite in sample 7-2-132 in Table 3). Electron microprobe major element analyses are used to distinguish between pure mica analyses and those of mixtures of mica with other phases (e.g., by examining total normalized K per 11 oxygens).

Table 2
Representative electron and ion microprobe data for white micas in Catalina Schist metasedimentary rocks

Spot	132WM6	32AWM2	312WM5	33WM	43WM	53MU1RE1	25WM2	GB1WM	324WM
Sample	7-2-132	6-2-32A	7-3-1′	8-2-33	7-3-43	6-3-53	6-3-25A	GB1	6-3-24
Grade	LA	LBS	LBS	EBS	EA	EA	AM	AM	AM–pegmatite
SiO_2	53.42	52.55	53.29	52.32	48.76	49.73	47.05	46.36	46.12
MgO	2.93	4.63	5.13	3.58	2.82	2.49	1.33	1.31	1.53
Na_2O	0.05	0.03	0.06	0.11	0.26	0.63	1.63	1.69	1.22
Al_2O_3	25.25	23.73	22.84	24.86	27.88	30.22	35.33	33.92	33.17
FeO	3.37	4.33	3.22	4.13	3.21	2.02	0.89	0.91	1.23
MnO	0.00	0.07	0.03	0.04	0.02	0.00	0.00	0.02	0.00
Cr_2O_3	0.01	0.03	0.07	0.11	0.02	0.05	0.00	0.03	
K_2O	10.33	10.25	9.92	9.50	10.58	10.31	8.68	9.01	9.49
CaO	0.00	0.01	0.03	0.11	0.02	0.01	0.00	0.01	0.01
TiO_2	0.06	0.08	0.05	0.05	0.30	0.44	0.68	0.57	1.17
Total	95.40	95.71	94.63	94.80	93.87	95.85	95.65	93.79	93.97
Normalized major element data (on basis of 11 oxygens)									
SiIV	3.553	3.517	3.577	3.511	3.327	3.292	3.09	3.116	3.108
AlIV	0.447	0.483	0.423	0.489	0.673	0.708	0.91	0.884	0.892
AlVI	1.532	1.389	1.383	1.478	1.569	1.651	1.824	1.803	1.742
Mg	0.291	0.462	0.514	0.358	0.286	0.246	0.131	0.131	0.154
FeT	0.187	0.243	0.181	0.232	0.183	0.112	0.049	0.051	0.069
Mn	0	0.004	0.002	0.002	0.001	0	0	0.001	0
Cr	0	0.001	0.003	0.006	0.001	0	0.003	0	0.002
TiVI	0.003	0.004	0.002	0.003	0.015	0.022	0.034	0.029	0.059
Total Y site	2.013	2.102	2.085	2.078	2.057	2.03	2.041	2.015	2.026
Ca	0	0.001	0.002	0.008	0.001	0.001	0	0.001	0.001
Na	0.006	0.003	0.008	0.014	0.035	0.081	0.207	0.22	0.159
K	0.876	0.875	0.849	0.813	0.921	0.871	0.727	0.772	0.816
Total X site	0.883	0.88	0.859	0.835	0.957	0.952	0.935	0.993	0.976
SIMS data (ppm)									
Li	10.5	12.4	25.0	47.7	56.5	52.9	39.4	16.8	70.8
B	178	119	125	77	49	44	54	25	16
Rb	260	248	236	235	235	262	105	132	124
Sr	4.8	2.7	3.9	15	39	386	364	432	199
Y	0.3	0.7	1.1	0.2	0.0	0.2	0.1	0.1	0.1
Zr	2.6	2.5	2.0	1.1	0.0	0.2	1.0	0.6	2.2
Cs	17.4	10.5	9.8	11.8	3.8	6.0	0.7	1.3	1.4
Ba	2433	3658	2420	1765	1749	1694	8473	1886	4673
Ce	0.4	0.0	0.1	0.0	0.0	0.0	0.0	0.0	0.0

Increasing grade from left to right; full dataset available from the authors upon request.
Grades: LA = lawsonite–albite; LBS = lawsonite–blueschist; EBS = epidote–blueschist; EA = epidote–amphibolite; AM = amphibolite.

3.2. Lithium

Lithium is primarily concentrated in chlorites and white micas, with chlorite containing somewhat higher concentrations of Li than coexisting white mica, while amphiboles also have variably high Li concentrations in some samples (see Fig. 3B; representative ion microprobe data for chlorite in Table 3). It is important to note that, in rocks of grades higher than epidote–blueschist (epidote–amphibolite and amphibolite), at least some of the chlorite is clearly retrograde in origin based on textural observations. Garnet in the higher-grade rocks incorporates significant amounts of Li, with concentrations of up to ~10 ppm. Bebout et al. (2004) noted Li concentrations of up to ~100 ppm, and strong core to rim decrease in Li concentration, in some UHP garnet in metasedimentary rocks from Lago di Cignana.

3.3. LILE (Cs, Ba, Rb, Sr)

The LILE concentrations in the Catalina Schist metasedimentary micas show diverse behavior

Table 3
Representative ion microprobe analyses of phases in metasedimentary rocks of the Catalina Schist

Spot	132CHL	94ACHL2	84ACZ2	25CZ	681LAW3	312LAW2	54GT	53GT2	312PL2	33PLAG5	53PLAG2
Sample	7-2-132	329-4A	328-4A	6-3-25A	6-5-68	7-3-1′	6-3-54	6-3-53	7-3-1′	8-2-33	6-3-53
Mineral	CHL	CHL	CZ	CZ	LAW	LAW	GT	GT	PL	PL	PL
Grade	LA	EBS	EBS	AM	LBS	LBS	EA	EA	LBS	EBS	EA
Element (concentration in ppm)											
Li	68.65	41.87	0.16	0.05	0.87	0.77	3.22	7.74	0.03	0.27	0.13
B	0.41	0.65	0.35	0.73	5.95	5.50	0.50	0.26	0.48	3.06	1.35
Rb	0.89	0.41	0.00	0.00	0.00	0.00	0.00	0.00	0.00	0.01	0.69
Sr	0.15	0.63	2010	3989	638	12857	0.9	0.2	35.4	18.39	141.44
Y	0.01	0.02	127	94	75	16053	97	60	0.0	0.13	0.03
Zr	0.13	0.08	11.01	7.29	11.5	69.7	1.16	4.99	0.06	0.18	0.14
Cs	0.00	0.01	0.08	0.04	0.00	2.99	0.01	0.01	0.04	0.00	0.04
Ba	4.72*	0.5	1.8	137.3	17.6	74.5	3.3	1.7	3.9	23.8	176.0
Ce	0.01	0.01	0.94	0.44	21.8	50927	0.07	0.00	0.00	0.07	0.02

Grades: LA = lawsonite–albite; LBS = lawsonite–blueschist; EBS = epidote–blueschist; EA = epidote–amphibolite; AM = amphibolite.
Minerals: CHL = chlorite; CZ = clinozoisite; LAW = lawsonite; GT = garnet; PL = plagioclase.
*Elevated Ba concentration likely due to very minor intermixture of white mica; Ba data for white mica for same sample in Table 2.

consistent with their varying charge and ionic radii relative to Ca and K. However, for all but Sr, the whole-rock element behavior can be represented well using the data for the micas (see discussions below). For Cs, Ba, and Rb, the white micas (and in a couple of higher-grade samples, biotite also) are the primary mineral hosts, with concentrations in white micas exceeding those of the whole-rock samples (Fig. 3C–F). Although plagioclase is a significant Ba host in the higher-grade rocks (~100 ppm in some samples), these concentrations amount to less than 5% of the Ba inventory in all but one of these samples with higher plagioclase Ba concentration, several of which are pegmatites or leucosomes from ampibolite-facies metasedimentary exposures.

For Sr, white-mica concentrations are significantly lower than the whole-rock concentrations at lower grades, and similar to the whole-rock concentrations at higher grades (Fig. 3F). Strontium is also strongly concentrated in calcium-rich phases such as An-rich plagioclase (see Figs. 2 and 3), lawsonite, clinozoisite, and titanite (and at lower grades, probably also calcite and aragonite, which were not analyzed in this study; representative ion probe data in Table 3). Thus, Sr has a somewhat more complex whole-rock distribution that reflects significant redistribution during prograde reaction history as these other Ca-rich phases were stabilized or destabilized. This is particularly evident at the lower grades, where the presence of lawsonite, some with Sr concentrations >10,000 ppm, resulted in white-mica Sr concentration significantly lower than the whole-rock concentrations.

3.4. Other trace elements (Zr, Ce, Y)

Because this project was designed mostly to evaluate mineral residency of the elements discussed above, and because the concentrations of Y, Ce, and Zr are all extremely low (at or below detection limits) in the phases in which B, Li, and the LILE are sited (see Table 2), we provide here only a very brief discussion of the residency of these remaining three elements. As expected, Zr abundance is highly influenced by the presence or absence of zircon, and occasional fluctuations to higher Zr during analyses of minerals thought to be nominally Zr-free likely reflect the ablation of micro-inclusions of zircon. Garnet strongly sequesters heavy REE and thus in these rocks contains only minor Ce; clinozoisite and lawsonite are significant REE hosts, generally showing enrichment in light REE (as illustrated by representative data for Ce in Table 3). Yttrium is present at significant concentrations in clinozoisite, lawsonite, and garnet (see discussion of Y partitioning in Otamendi et al., 2002; King et al., 2004).

4. Discussion

4.1. Evidence for trace element redistribution and loss during devolatilization

The results presented here demonstrate the complexity of trace element redistribution during prograde metamorphic history, as fluid/bulk-rock partitioning evolves in response to metamorphic mineral reactions

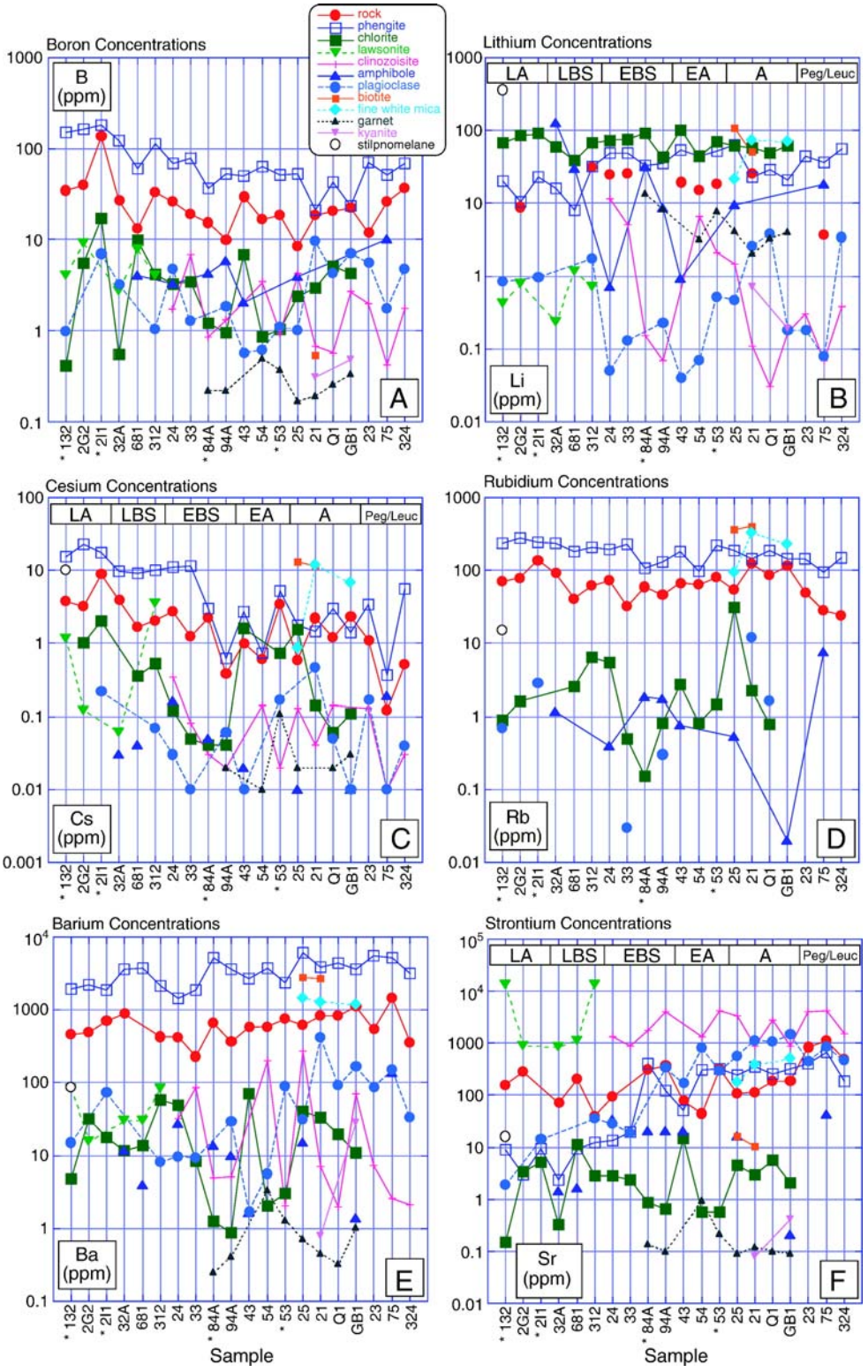
rock
phengite
chlorite
lawsonite
clinozoisite
amphibole
plagioclase
biotite
fine white mica
garnet
kyanite
stilpnomelane
Boron Concentrations
B (ppm)
A
Lithium Concentrations
LA
LBS
EBS
EA
A
Peg/Leuc
Li (ppm)
B
Cesium Concentrations
Cs (ppm)
C
Rubidium Concentrations
Rb (ppm)
D
Barium Concentrations
Ba (ppm)
E
Strontium Concentrations
Sr (ppm)
F
* 132
2G2
* 2I1
32A
681
312
24
33
* 84A
94A
43
54
* 53
25
21
Q1
GB1
23
75
324
Sample

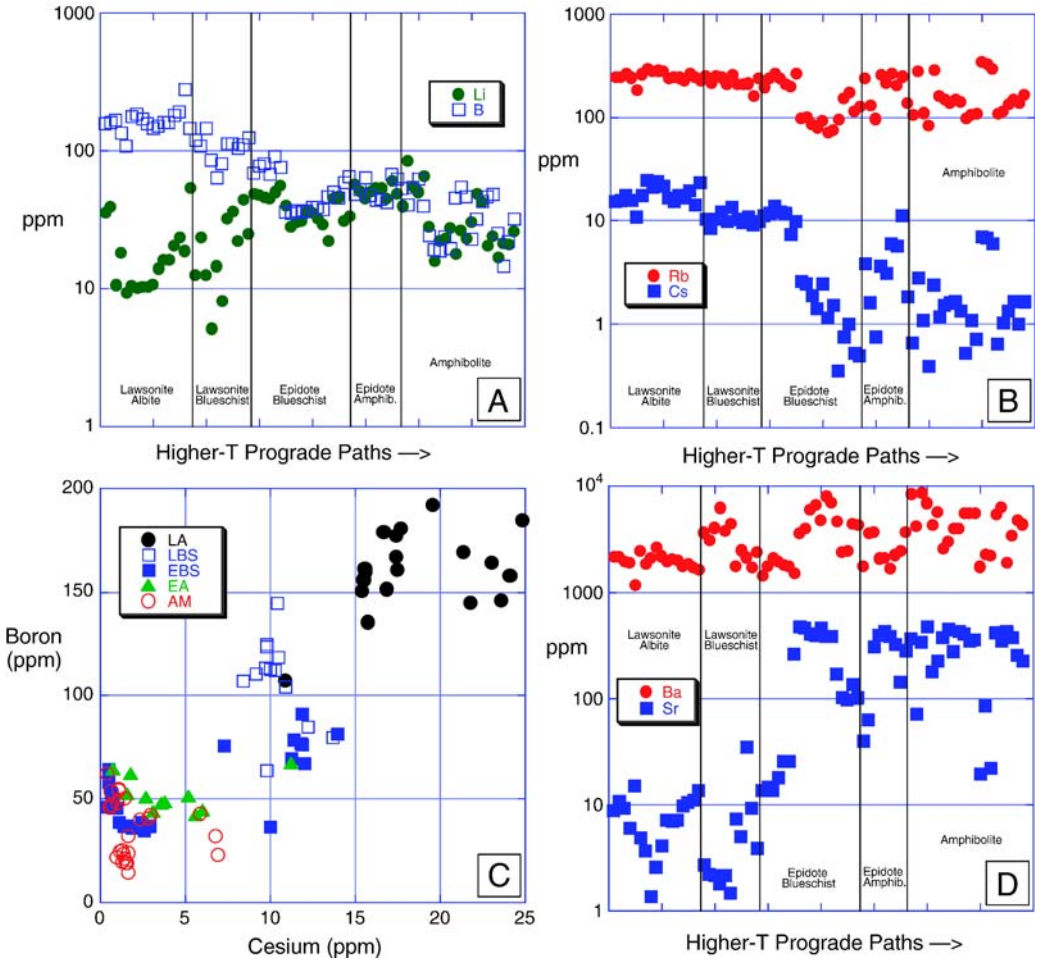

Fig. 4. Variations of concentrations of B, Li, Cs, Rb, Ba, and Sr in white micas in metasedimentary rocks (data for pegmatites and leucosomes, shown in Fig. 3, are not included) with increasing metamorphic grade (to the right). In these plots, the samples within each grade are ordered as in Fig. 3. (A) Plot of B and Li white-mica concentrations vs. grade, demonstrating the lower white-mica B concentrations, and higher white-mica Li concentrations, in rocks experiencing paths into metamorphic grades of epidote–blueschist and higher. (B) Plot of Rb and Cs white-mica concentrations vs. grade, demonstrating relatively uniform Rb concentrations across grades, and lower Cs concentrations in white micas in rocks experiencing paths into metamorphic grades of epidote–blueschist and higher. Note the greater scatter in the Rb concentrations in the higher-grade units, presumably related to partitioning of some Rb into biotite at varying modal abundance. (C) Plot of Cs vs. B in white micas in the Catalina Schist metasedimentary rocks, demonstrating correlated decreases in concentration in higher-grade units. (D) Plot of Ba and Sr white-mica concentrations vs. grade, demonstrating relatively uniform Ba concentrations across grades, and higher Sr concentrations in white micas in rocks experiencing paths into metamorphic grades of epidote–blueschist and higher. Note the greater scatter in the Ba concentrations in the higher-grade units, presumably related to partitioning of some Ba into biotite at varying modal abundance. Note that these plots do not include data for fine-grained white mica believed to be retrograde in origin based on textures and mineral chemistry (see text for discussion).

with changing pressure and temperature. Many of these reactions are continuous, involving changes in mineral chemistry and modal abundance without change in mineral assemblage. Ion microprobe and bulk analyses of the principal metamorphic minerals indicate that B, Cs, Rb, and Ba are largely hosted by the micas in the metasedimentary rocks (Fig. 3; see previous discussions by Moran et al., 1992; Bebout et al., 1993; Moran, 1993;

Fig. 3. A–F. Average concentrations of B, Li, and LILE (Rb, Sr, Cs, Ba) in coexisting minerals in metasedimentary rocks and leucosomes/pegmatites (the latter, samples “23”, “75”, and “324” on the right side of each figure) of the Catalina Schist (obtained by SIMS methods), arranged in order of increasing metamorphic grade from left to right. Lines connecting data for the same mineral across grade emphasize the systematic nature of the trace element distributions. Asterisks indicate samples containing tourmaline. Boundaries between metamorphic grades are indicated on (B), (C), and (F). In this and later figures, abbreviations for metamorphic grade are the same as in Fig. 1.

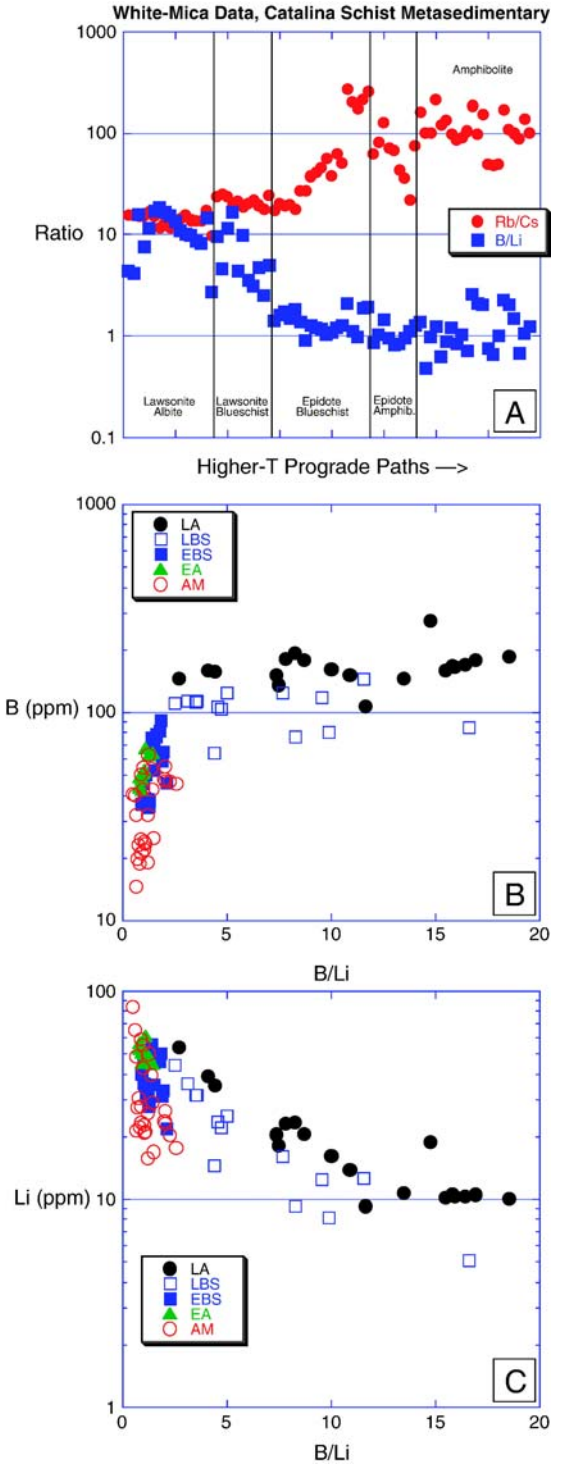

Fig. 5. Demonstration of changes in white mica Rb/Cs and B/Li with increasing metamorphic grade (A), and the dependence of changing B/Li on both decreasing B concentration (B) and increasing Li concentration (C). Note that these plots do not include data for fine-grained white mica believed to be retrograde in origin based on textures and mineral chemistry (see text for discussion).

Domanik et al., 1993; Bebout et al., 1999; Melzer and Wünder, 2001a,b; Zack et al., 2001; Busigny et al., 2003), whereas Li and Sr show more complex mineral residency also involving other modally significant phases (for Li, chlorite; for Sr, carbonates, lawsonite, clinozoisite, and plagioclase). Particularly for Rb and Cs, greater scatter in concentrations in white mica at the higher grades probably reflects partitioning of these elements into biotite present at varying modal proportions; however, the decrease in Cs concentrations is known to be reflected also in the whole-rock data, seemingly indicating whole-rock Cs loss during devolatilization (see Bebout et al., 1993, 1999). Interestingly, although this suite of trace elements is largely housed in the white micas, the elements reside in several quite different crystallographic sites in the micas. Boron is known to be housed in tetrahedral sites in the micas, whereas K and the other LILE are sited in the interlayer sites and Li is likely in octahedral sites due to its similarity in ionic radius to Mg. In a related study of N behavior during devolatilization of the Catalina Schist metasedimentary suite, Bebout and Fogel (1992; also see Bebout, 1997) documented the correspondence of whole-rock N and K_2O concentrations reflecting the residence of N in the micas as NH_4^+, presumably also in interlayer sites.

It has been suggested in recent studies that the thermal structure of subduction zones influences the efficiency with which volatile components are deeply subducted (Abbott and Lyle, 1984; Bebout, 1991a; Staudigel and King, 1992; Moran et al., 1992; Bebout et al., 1993, 1999; Kirby et al., 1996; Busigny et al., 2003). Cooler subduction-zone thermal regimes (those in which relatively old oceanic lithosphere is being relatively rapidly subducted; Kirby et al., 1996; Peacock, 1996) are thought to promote the deep retention of volatiles, perhaps increasing the contributions of volatile components to the deep mantle, including arc lava source regions (see Bebout et al., 1999; Sadofsky and Bebout, 2003). In the Catalina Schist metasedimentary rocks, devolatilization reactions released H_2O-rich C–O–H–S–N fluids (Bebout, 1991a; Bebout and Fogel, 1992; Bebout and Barton, 1993; Bebout et al., 1993, 1999). H_2O contents in the rocks decrease from 3–5 wt.% in the lowest-grade, lawsonite–albite facies rocks to 1–3 wt.% in the highest-grade, amphibolite-facies rocks. At all grades, more aluminous rocks have the highest H_2O contents (Bebout, 1995). This loss is attributable to breakdown of chlorite and phengitic white mica to stabilize muscovite, biotite, garnet, and kyanite (Fig. 2; for generalized reactions see Bebout and Fogel, 1992; Bebout et al., 1993, 1999). The highest-grade,

amphibolite-facies metasedimentary rocks are believed to have experienced H_2O-saturated partial melting resulting in the production of quartz+plagioclase±muscovite leucosomes and pegmatites (Bebout and Barton, 1993) —their volatile and trace element concentrations thus reflect the combined effects of subsolidus devolatilization and partial melting. Increases in $\delta^{15}N$ and decreases in N concentration in the higher-grade rocks relative to their likely seafloor sediment protoliths are consistent with devolatilization and loss, to fluids, of N_2 with $\delta^{15}N$ lower than that of the rocks (see Bebout et al., 1999), perhaps during a devolatilization process approximating Rayleigh distillation (Bebout and Fogel, 1992; discussion of B isotope data by Bebout and Nakamura, 2003). It is important to note that the lower-grade rocks, because of their contrasting prograde *P–T* paths relative to the high-grade rocks, are not directly representative of the earlier stages of devolatilization of the higher-grade rocks. However, the lowest-grade (lawsonite–albite-facies) metasedimentary rocks in the Catalina Schist are broadly similar, in volatile contents and major and trace element compositions, to seafloor sediments in modern trench settings (Bebout and Fogel, 1992; Bebout et al., 1993, 1999) and are therefore used as a proxy for the protoliths of the higher-grade metasedimentary rocks.

Bebout and Fogel (1992) and Bebout et al. (1999) examined the effects of varying major element composition on whole-rock trace element concentration. At any single metamorphic grade, whole-rock K_2O contents correlate with the concentrations of B, Cs, N, Rb, and Ba, reflecting the principal residence of these trace elements in micas (the only significant K_2O-bearing mineral in the rocks; see Figs. 2 and 3). Whole-rock Cs/K_2O and B/K_2O (and N/K_2O), presumably reflecting the concentrations of these trace elements in the micas, are significantly lower in the epidote–amphibolite and amphibolite facies rocks than in the lower-grade equivalents. However, whole-rock K_2O, Ba, and Rb (strongly concentrated in micas), Sr (hosted in micas, but also in lawsonite and clinozoisite and, in the lowest-grade rocks, in finely disseminated carbonate; Bebout, 1995), and Li (hosted in micas, but also in chlorite and occasionally in amphibole) do not show obvious decreases with increasing metamorphic grade. The differences in behavior between B, Cs, and N and these other elements presumably reflect differential partitioning of these elements into aqueous metamorphic fluids during devolatilization reactions (also see Melzer and Wünder, 2001a,b; Zack et al., 2001).

The effect of increasingly high-*T* prograde metamorphic history on the B and Cs concentrations in the Catalina Schist metasedimentary rocks demonstrated by Bebout et al. (1999) with whole-rock Cs/K_2O and B/K_2O ratios, is borne out by examination of the B and Cs concentrations in white micas in the same rocks (see Figs. 3–8). Concentrations of B and Cs in white micas in the higher-grade units are significantly lower than concentrations in the low-grade units, whereas white-mica Rb and Ba concentrations show no significant change with increasing grade, and white-mica Sr and Li concentrations show increase with increasing grade (Fig. 4). The most dramatic decreases in B and Cs concentration in white mica occur in rocks which experienced prograde paths into the epidote–blueschist or higher grades. Rocks of these higher grades exhibit enrichments in Li and Sr in white mica that are believed to have resulted from destabilization of chlorite, carbonates, and lawsonite (Fig. 4A,D). In rocks which

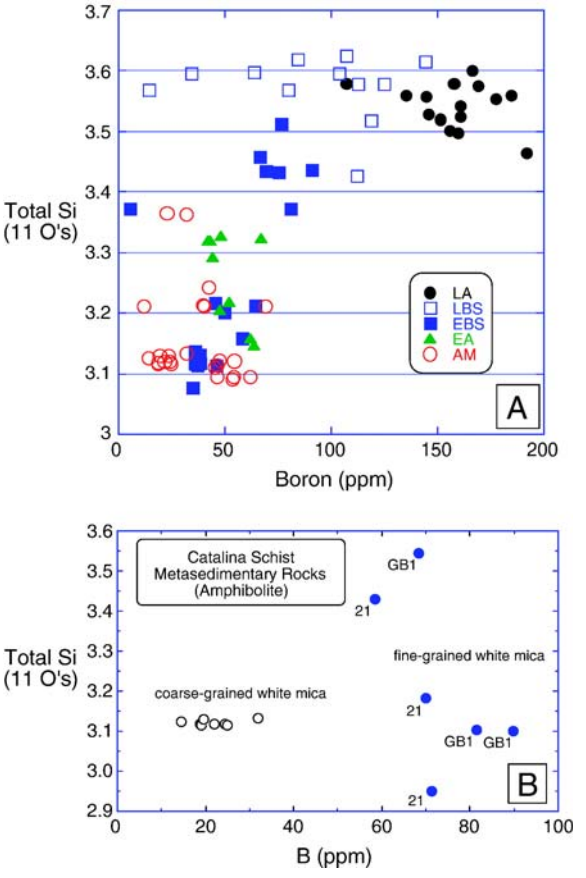

Fig. 6. Relationship of white mica B concentration with total Si (on the basis of 11 oxygens) for metasedimentary rocks of the Catalina Schist (A). Demonstration of the contrasting trace element compositions of "prograde" (coarse-grained, low-Si) and "retrograde" (fine-grained, mostly higher-Si) generations of white micas in two amphibolite-grade metasedimentary samples (B). Note that (A) does not include data for fine-grained white mica believed to be retrograde in origin.

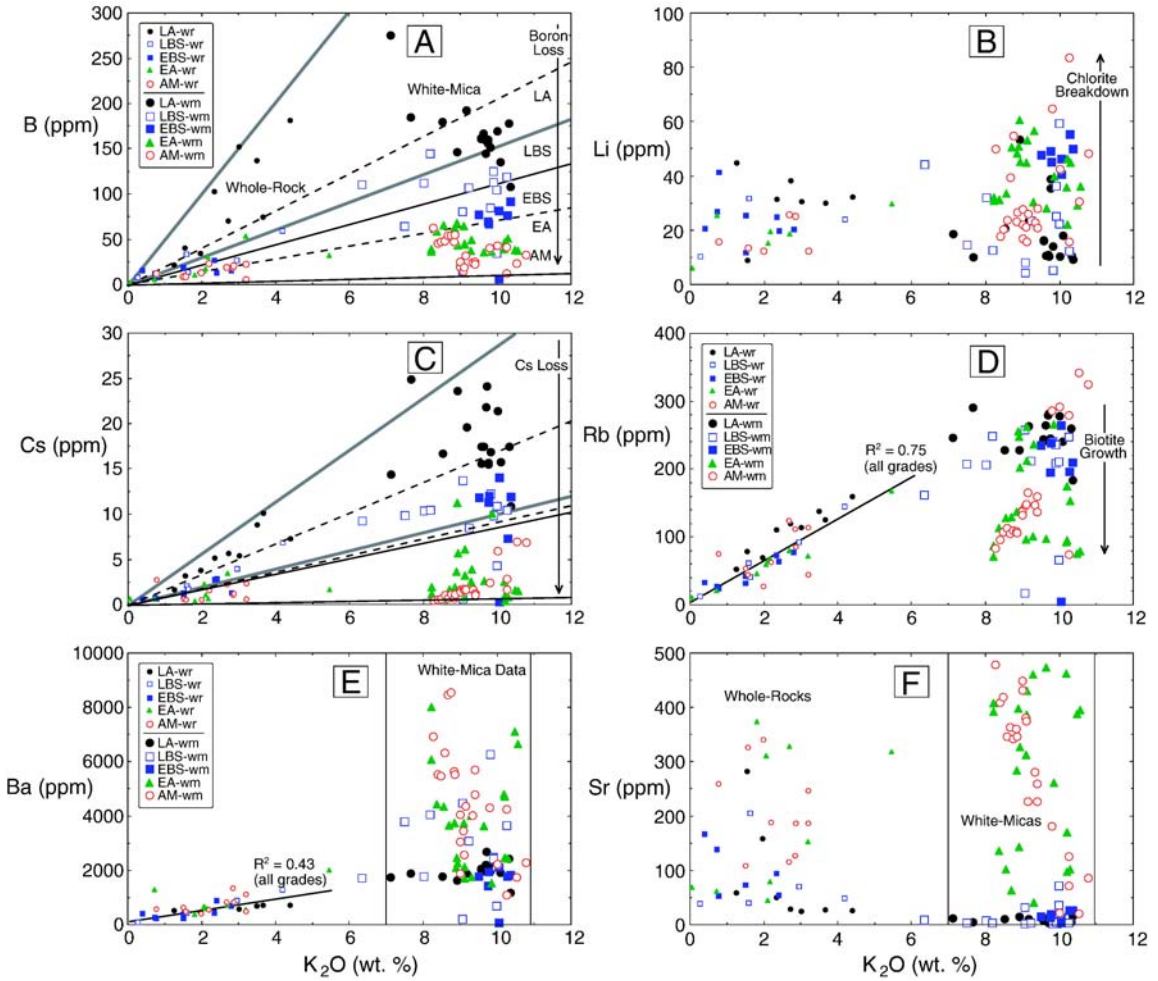

Fig. 7. Relationships between whole-rock and white-mica K_2O and trace element concentrations. Note that Rb and Ba show the strongest whole-rock correlations with K_2O concentration (D, E). Sr and Li concentrations do not correlate with K_2O content, as these elements are also strongly partitioned into other phases (for Li, chlorite; for Sr, lawsonite, clinozoisite, and minor carbonate and titanite; B, F). Boron and Cs whole-rock concentrations correlated with K_2O concentration and data for higher-grade units indicate loss of B and Cs relative to K_2O during devolatilization reactions (A, C). Note that these plots do not include data for fine-grained white mica believed to be retrograde in origin based on textures and mineral chemistry (see text for discussion). In A and C, diagonal lines for the lawsonite–albite facies (thicker patterned lines), lawsonite–blueschist facies (dashed lines), and amphibolite facies (thinner lines) represent boundaries of zones within which whole-rock compositions can be explained by dilution of white micas as the sole mineral host for B and Cs, respectively, by other phases not containing these elements (e.g., quartz, chlorite). Note that, for each of the three grades, nearly all of the white micas fall within these zones.

experienced the *P–T* paths into the lawsonite–albite and lawsonite–blueschist facies, whole-rock and white-mica concentrations of the elements strongly partitioned into micas (particularly Rb and Cs) appear to strongly resemble seafloor sediment protoliths (see Fig. 8). In white micas, losses of B and Cs relative to Li and Rb, with increasing grade, result in decreases in B/Li and increases in Rb/Cs (see Figs. 4A–C and 5). For the Rb/Cs ratios, the increases can be directly related to decreases in the concentrations of Cs at relatively constant Rb concentration (see Figs. 4A and 5A). B/Li ratios of micas in the higher-grade metasedimentary rocks are in part a result of increases in Li concentration (see Fig. 5C), thought to be related to the breakdown of chlorite, the primary Li host at lower grades (see Figs. 2 and 3B).

Fig. 6A illustrates the relationship between B concentrations in white micas with the Si content of the same micas, with the decrease in total Si (on the basis of 11 oxygens) reflecting peak recrystallization over the wide range in grade (see Sorensen, 1986; see Fig. 2). In the higher-grade rocks, textures and mineral chemistry were used to distinguish the white micas better preserving prograde metamorphic compositions

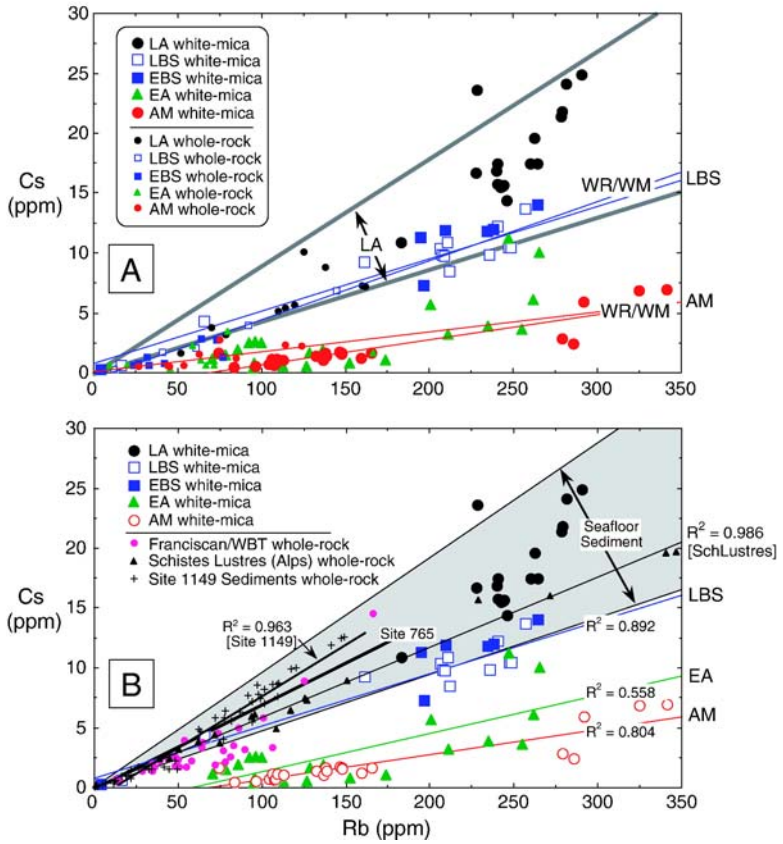

Fig. 8. Rb–Cs concentrations of seafloor sediments, Catalina Schist whole-rock metasedimentary samples and white micas, and the Schistes Lustrés metasedimentary suite. (A) Comparison of whole-rock and white-mica Rb–Cs compositions for metasedimentary rocks of the Catalina Schist (whole-rock data from Bebout et al., 1999). Note the compatibility of whole-rock and white-mica concentrations for these elements, which are strongly partitioned into micas as the only significant potassic mineral phase. As a demonstration, this plot includes comparisons of separate linear regressions through the whole-rock and the white-mica data for the lawsonite–blueschist facies and amphibolite facies samples (pairs of lines labeled, "WR/WM"). For the lawsonite–albite facies samples, the two black lines represent the zone within which the whole-rock compositions can be explained by dilution of white micas as the sole host for Rb and Cs, by other phases not containing these elements. (B) Comparison of Catalina Schist Rb–Cs white-mica compositions with the range of Rb/Cs of seafloor sediments (shaded region labeled, "Seafloor Sediment"), the latter from Ben Othman et al. (1989) and Plank and Langmuir (1998; seafloor sediment from ODP Sites 765 (Banda forearc; linear regression shown only) and 1149 (Izu–Bonin; web citations for both sites; T. Plank and K. Kelley, personal communication). Also shown, for comparison, are data for Franciscan and Western Baja Terrane metasedimentary rocks (from Sadofsky and Bebout, 2003) and for the Schistes Lustrés (from Busigny et al., 2003). Note that these plots do not include data for fine-grained white mica believed to be retrograde in origin based on textures and mineral chemistry (see text for discussion). Linear regressions (labeled lines with values for R^2) are provided for the white micas in the lawsonite–blueschist, epidote–amphibolite, and amphibolite facies Catalina Schist metasedimentary rocks, and for the Schistes Lustrés (labeled, "SchLustres").

from those more obviously related to recrystallization during exhumation and cooling (see example of distinct compositions in Fig. 6B). The Si content of potassic white micas increases with increasing water pressures and decreasing temperatures, with maximum Si contents at any *P–T* occurring in appropriately buffered assemblages. Some fine-grained retrograde white micas have high Si contents, probably reflecting the low temperatures but continuing high pressures of retrogressive alteration (see discussion of accretionary history and *P–T* paths in Grove and Bebout, 1995). Plots of B and Cs concentrations versus K_2O content for the whole-rocks and white micas (Fig. 7A,C) demonstrate the correspondence of B and Cs whole-rock concentrations with the abundance and B–Cs contents of white mica, which serve as the only significant K-rich phase in these rocks. Also evident on these plots is the loss of B and Cs resulting in lowered B/K_2O and Cs/K_2O in both the whole-rocks and white micas. Similar plots for Li, Rb, Ba, and Sr, demonstrate more complicated patterns. For Rb and Ba, whole-rock data for all units combined produce a linear array without any dependence on grade

(Fig. 7D,E), whereas Li and Sr show more erratic concentrations (Fig. 7B,F), overlapping among grades, apparently related to the strong partitioning of these elements also into other, non-potassic phases (for Li, chlorite; for Sr, lawsonite, clinozoisite, and minor carbonate and titanite).

4.2. Comparison with other observations regarding LILE mobility during high-P/T metamorphism

Relatively few studies have been conducted on devolatilization across metamorphic grade in subducted metasedimentary rocks (this study; Sadofsky and Bebout, 2003; Busigny et al., 2003; for N only, see Mingram and Brauer, 2001), whereas a number of recent studies have examined evidence for trace element redistribution and loss in HP and UHP metamafic rocks (e.g., Spandler et al., 2004; King et al., 2004; Usui et al., 2006). A study by Sadofsky and Bebout (2003; also see studies of paleoaccretionary fluid mobility by Sadofsky and Bebout, 2001, 2004) endeavored to identify any subtle disruption in C–N-isotope signatures (organic component) and trace element budgets in metaclastic rocks subducted to depths of ~5–50 km, utilizing exposures of the Franciscan Complex, Western Baja Terrane, and the Catalina Schist (simplified *P–T* conditions in Fig. 1; Franciscan at low-*T* end of Catalina *P–T* range). Despite significant loss of H_2O during clay-to-mica and other reactions, trace element concentrations show little change (for even relatively "fluid-mobile" elements such as B, Cs, As, and Sb).

Busigny et al. (2003) presented data for whole-rocks and white mica separates indicating that phengite may convey LILE, H, and N to depths of up to ~90 km in cooler subduction zones. In their study of a traverse of the Schistes Lustrés in the Cottian Alps, Italy, previously studied by Agard et al. (2002), these authors demonstrated relatively uniform average concentrations (and for N, stable isotope composition) and constant element ratios (Cs/Rb, K/Cs, and Rb/N) across a wide range in metamorphic grade, indicating that these metasedimentary rocks behaved as closed systems during subduction. In a separate study focusing on SIMS mineral analyses, for samples across the same traverse, Bebout et al. (2003, 2004) demonstrated the stable coexistence of phengite and paragonite (and related complex partitioning of mica-hosted trace elements) in higher-grade samples from the localities studied by Busigny et al. (2003). There is considerable variation in the trace element compositions of white micas in single samples, perhaps related to varying recrystallization during the exhumation known to have affected these rocks (cf. Reinecke, 1998; Agard et al., 2002). Although these rocks are variably to extensively overprinted by exhumation, this dataset provides an intriguing indication that these elements are efficiently retained in mica-bearing rocks metamorphosed along low-*T* prograde *P–T* paths (cf. Busigny et al., 2003), and a suggestion that much of the subducted mica-borne LILE and N inventory could be available to the depths beneath arc volcanic fronts (global average of ~100 km; see Syracuse and Abers, 2006). This apparent retention of N to near sub-arc depths is relevant to considerations of N return in arc volcanic gases, and the arguments regarding the efficiency of return of the subducted seafloor N inventory to the surface via arc volcanism (see Fischer et al., 2002; Sadofsky and Bebout, 2004; Li and Bebout, 2005).

Melzer and Wünder (2001a,b), Zack et al. (2001), and Busigny et al. (2003) have recently considered fluid-mica partitioning (in each case with some discussion of the data for the Catalina Schist metasedimentary rocks), and the extent to which concentration data for elements such as Rb, Cs, and Ba for metamorphic suites can be used to calculate fluid compositions or rock element losses as a function of *P* and *T* and other factors such as chlorinity (also see consideration of K, Rb, Cs, and N fluid-mica partitioning by Busigny et al., 2003). These elements are well-suited for this approach because of their extreme partitioning into phengite in both metasedimentary and metamafic bulk compositions (see Domanik et al., 1993; Zack et al., 2001). Although the exact magnitudes of the calculated loss of relatively fluid-mobile elements is debated and known to depend on the applicability and quality of experimental data and the models of release (see Zack et al., 2001; Busigny et al., 2003), there is general agreement regarding the relative degrees of mobilization of such elements in aqueous fluids (Cs > Ba > Rb); thus reduced Cs/Rb and Ba/Rb are predicted by the devolatilization models of Zack et al., 2001). Of these three elements, only Cs is demonstrably reduced at higher grades in the Catalina Schist; the identification of loss of any element is complicated by the large degrees of heterogeneity for the higher-grade rocks and their presumed protoliths. However, in the work on the Catalina Schist metasedimentary rocks, B and N have also been demonstrated as being mobilized and reduced in concentration in more devolatilized, higher-grade rocks (this study, Bebout et al., 1993, 1999).

Fig. 8 provides a comparison of Rb–Cs systematics in seafloor sediments, whole-rocks and white micas of varying grades in the Catalina Schist, low-grade Franciscan Complex and Western Baja Terrane whole-

rock metasedimentary samples, and rocks of the Schistes Lustrés. Fig. 8A demonstrates the correspondence of whole-rock and white-mica Cs/Rb for rocks at individual grades in the Catalina Schist (note the very similar linear regressions through the whole-rock and white-mica data for both the lawsonite–blueschist grade and the amphibolite grade rocks), again demonstrating that the inventories of these elements in these rocks are controlled by the white micas. In Fig. 8B, it is evident that the low-grade Catalina Schist white micas and the Schistes Lustrés whole-rocks (data for the latter from Busigny et al., 2003) have Rb–Cs compositions similar to those of seafloor sediments, whereas the higher-grade units of the Catalina Schist (epidote–amphibolite and amphibolite facies) have lower Cs/Rb believed to be related to greater degrees of devolatilization. Chlorite is absent as a prograde phase in epidote–amphibolite and amphibolite facies metasedimentary rocks in the Catalina Schist, but is stable across the traverse of the Schistes Lustrés sampled by Busigny et al. (2003). Dehydration and resulting reaction-enhanced permeability may contribute to the open-system behavior of the higher-grade Catalina Schist metasedimentary rocks, promoting fluid loss or infiltration, whereas the Schistes Lustrés and lower-grade Catalina Schist metasedimentary rocks appear to have behaved as closed systems to LILE loss or gain.

4.3. Compatibility with other chemical trends observed in and across forearcs and arcs

Forearc metamorphic suites such as the Catalina Schist (and Franciscan Complex) are dominantly composed of the terrigenous sedimentary lithologies (greywacke, shale) thought to dominate the subducted sedimentary inventory (cf. Plank and Langmuir, 1993, 1998; Sadofsky and Bebout, 2003). The lithology of deeply subducted sediment sections varies significantly among modern subduction zones (see compilations by Rea and Ruff, 1996; Plank and Langmuir, 1998), and complex relationships among subduction accretion/underplating and erosion influence the nature and magnitude of subduction of "continental" materials (see von Huene and Scholl, 1991) influencing geochemical evolution at depth in subduction zones. However, we provide here a brief discussion of compatibilities between the records of element mobilization in forearc metamorphic suites and the evidence for their mobility from study of accretionary prism fluids, forearc serpentinite seamounts in the Marianas margin, and arc volcanic rocks (including across-arc suites; also see Bebout, in press).

You et al. (1995, 1996) presented the results of fluid–sediment experiments, at various fluid–rock ratios, which demonstrated trace element release broadly compatible with observations in the Catalina Schist. These experiments were conducted at temperatures similar to those experienced by the low-grade units of the Catalina Schist (<300 °C), but at lower pressures (<0.1 GPa) and at higher fluid–rock ratios (water: rock = 3 by weight; You et al., 1996). These authors demonstrated that, at these high fluid–rock ratios, As, Ba, B, Cs, NH_4^+, Pb, and Rb could be relatively mobile in shallow parts of accretionary prisms in zones of enhanced fluid flux. In the Marianas margin, forearc serpentinite seamounts provide information regarding slab-to-surface fluxes (see Benton, 1997; Benton et al., 2001) that can be directly compared with metamorphic suites which experienced peak recrystallization at P–T conditions in the slab beneath the modern seamounts. Depths of 16–21 km to the slab–mantle interface were estimated by Fryer et al. (1995, 1999) for blueschist facies clasts from serpentinite seamounts, and Mottl et al. (2004) estimated depths of 16–29 km depths to the slab beneath the serpentinite seamounts for which they inferred additions of slab chemical components. Based on fluid compositions in these seamounts, Mottl et al. (2004) proposed element mobility that shows some agreement with the trends observed in the Catalina Schist. These authors noted increases in fluid Cs, Rb, Sr (particularly at shallow levels), K, and B concentrations as functions of inferred distance from the trench (and depth to the subducting sediment + slab section), and inferred the addition of these elements by fluids derived from the subduction section. The data for low-grade metasedimentary rocks in the Catalina Schist, Franciscan Complex, and Western Baja Terrane (this study; Sadofsky and Bebout, 2003) seemingly indicate that losses of these elements at these shallow levels are insufficient to impart observable change in their concentrations (and ratios among their concentrations) in the rock residues. Because of the great compositional heterogeneity of the sediment protoliths, element losses of 10% or greater due to forearc fluid expulsion and devolatilization reactions could certainly go undetected by the whole-rock and single-mineral analyses.

Additions from subducting sediment and altered oceanic crust are commonly invoked to explain the enrichments in arcs of elements such as Rb, Cs, Ba, B, and Li, in addition to Th, U, Pb, and ^{10}Be (see discussion by Morris and Ryan, 2003; George et al., 2005). Transfer of these elements into arc source regions is variably attributed to aqueous fluids, silicate melts, or supercritical fluids with properties approaching those of

silicate liquids (see discussions by Johnson and Plank, 1999; Manning, 2004; Kessel et al., 2005), and it is conceivable that the physicochemical properties of this transfer agent change as a function of pressure and temperature in the slab across arcs (discussions by Morris and Ryan, 2003; Kessel et al., 2005). It is important to note that, whereas the data presented here and in Bebout et al. (1993, 1999) provide an indication of the dependence of fluid loss on temperature in subduction zones to depths of 40 km (and perhaps up to 90 km, incorporating the results of Busigny et al., 2003), and of the trace element inventory that is subducted to these depths in most modern subduction zones, the observations from these forearc suites obviously do not directly represent the fluid–melt–mineral partitioning at depths beneath arcs (generally >100 km). The record of element losses in the Catalina Schist for B, and Cs (and As and Sb; Bebout et al., 1999) is, however, broadly compatible with the slab and sediment losses proposed to explain element enrichments in arc volcanic suites (see Bebout et al., 1999; Morris and Ryan, 2003; references therein), and the studies of the Catalina Schist metasedimentary rocks indicate relative immobility in aqueous fluids of elements such as Rb, Ba, Be, Th, and the LREE. As one example of the compatibility of the trends observed in our data and sediment-related enrichments in arcs, the release and addition to source regions of fluids with low Rb/Cs during devolatilization, producing an increase in the Rb/Cs of the subducting sediments, has been suggested as an explanation for the lowered Rb/Cs in island arc volcanic rocks relative to ratios in MORB and OIB (Hart and Reid, 1991; also see McDonough et al., 1992).

Across-arc geochemical variation (in trace element and stable isotope compositions) is in part attributed to progressive metamorphism of subducting sediment and altered oceanic crust (Ishikawa and Nakamura, 1994; Ryan et al., 1995, 1996; Noll et al., 1996; Ishikawa and Tera, 1997; Shibata and Nakamura, 1997; Moriguti and Nakamura, 1998; Ishikawa and Tera, 1999; Bebout et al., 1999; Ishikawa et al., 2001; Melzer and Wünder, 2001a,b; Rosner et al., 2003; Moriguti et al., 2004), pointing to some interesting tests of the compatibility of the metamorphic and arc geochemical records. The across-arc variations observed for ratios such as B/Be, B/La, and Cs/Th are interpreted by some as reflecting progressive loss (and resulting diminishing inputs) of B and Cs from metamorphosing slab and sediments (e.g., Ryan et al., 1995, 1996; Melzer and Wünder, 2000; Morris and Ryan, 2003), beginning at depths of ~100 km. The apparently efficient retention of the B–Cs–N inventory to depths of up to 90 km implied by study of high-P/T metasedimentary suites (this study; Busigny et al., 2003), in rocks experiencing relatively low-T prograde P–T paths in modern subduction zones, is consistent with the availability of this trace element inventory for progressive release into subarc regions, perhaps producing the across-arc trends.

B and Li have increasingly been used as tracers of slab inputs in arc lavas (Morris et al., 1990; Ishikawa and Nakamura, 1994; Ryan et al., 1995, 1996; Leeman, 1996; Smith et al., 1997; Ishikawa and Tera, 1997; Moriguti and Nakamura, 1998; Chan et al., 1999; Ishikawa and Tera, 1999; Tomascak et al., 2000; Ishikawa et al., 2001; Tomascak et al., 2002; Straub and Layne, 2003; Rosner et al., 2003), in part because of their enrichment in sediment and AOC and because they are regarded as being "fluid-mobile." Our data regarding behavior of these elements during prograde metamorphism can be directly compared with B–Li datasets for arc and across-arc suites (see also Bebout et al., 1993, 1999). For example, in a study of tourmaline in HP and UHP metasediments, Bebout and Nakamura (2003) proposed a model of B isotope fractionation that is compatible with variations seen across modern arcs (cf. Peacock and Hervig, 1999; Nakano and Nakamura, 2001). Zack et al. (2003) suggested that Li isotopes are fractionated by devolatilization in subducting basalts, influencing Li isotope signatures in forearcs and in arc lavas. However, the whole-rock Li concentrations in the Catalina Schist metasedimentary suite do not demonstrate loss across grade, with any possible loss obscured by the variation in Li concentrations among samples of similar grade (see data in Bebout et al., 1999). Data for white mica (Fig. 4A) similarly do not appear to show decrease in Li concentration with increasing grade. For Li, white-mica concentrations might be expected to *increase* with increasing grade, as chlorite, a significant Li host, breaks down, and the plots in Figs. 4A and 5C do show an increase in Li concentration with increasing grade.

4.4. Nature of the devolatilization process

Zack et al. (2001) concluded that, whereas the differential element loss indicated by the Catalina Schist metasedimentary rocks is compatible with published experimentally-derived fluid–mineral partition coefficients, the amount of fluid loss during devolatilization required to produce the measured element loss is considerably greater than that which could have been derived locally (based on the measured decrease in H_2O content across metamorphic grade in the Catalina suite provided by Bebout, 1995). Significant errors could exist in published fluid–mineral partition coefficients

(perhaps up to an order of magnitude; see Zack et al., 2001) or related to the use of partition coefficients obtained for pressures higher than those of the Catalina Schist metamorphism. However, if these partition coefficients are at least approximately applicable, it could be necessary to invoke some open-system behavior and stripping of the more mobile elements by infiltrating fluids (cf. Zack et al., 2001). Infiltration of these rocks, during prograde metamorphism, by H_2O-rich fluids previously equilibrated at lower temperatures, or with more LILE-poor lithologies such as devolatilizing oceanic crust or hydrated ultramafic rocks in the subducting plate (or mélange zones; see Bebout and Barton, 2002; Bebout, in press) could provide a mechanism for the enhanced scavenging of LILE from metasedimentary rocks. Previously published O-isotope data for the amphibolite-facies unit were interpreted as reflecting infiltration by aqueous fluids previously equilibrated with metasedimentary rocks at lower temperatures (see discussions by Bebout and Barton, 1989; Bebout, 1991a,b; Grove and Bebout, 1995). Although the O isotope data for some amphibolite-facies metasedimentary rocks away from more the permeable mélange zones appear to record smaller degrees of fluid–rock interaction, significant trace element scavenging by infiltrating fluids may have occurred without leaving an obvious O-isotope record of this fluid–rock interaction. Such infiltration, resulting in incremental loss of more fluid-mobile elements isotopically equilibrated with the residue, could produce changes in concentrations and isotopic compositions of B and N that resemble a Rayleigh distillation process (see Bebout and Fogel, 1992; Bebout and Nakamura, 2003).

Yet another mechanism for releasing relatively fluid-mobile elements from metasedimentary compositions, which the data in this paper for metasedimentary rocks do not address, could involve complex mechanical and metasomatic mixing in the abundant mélange exposed in some high-P/T metamorphic suites (Bebout and Barton, 2002; Breeding et al., 2004; King et al., 2006). Bebout and Barton (2002) suggested that depletions in Ba, Sr, and K in amphibolite-facies mélange could reflect stripping of these elements, by fluids, from mixtures of ultramafic, mafic, and sedimentary lithologies (also see King et al., 2006). Breeding et al. (2004) documented release of metasedimentary trace elements related to metasomatic exchange between sedimentary blocks and ultramafic mélange matrix, and proposed that this is an important mechanism in delivering the slab+sediment trace element inventory to arc source regions.

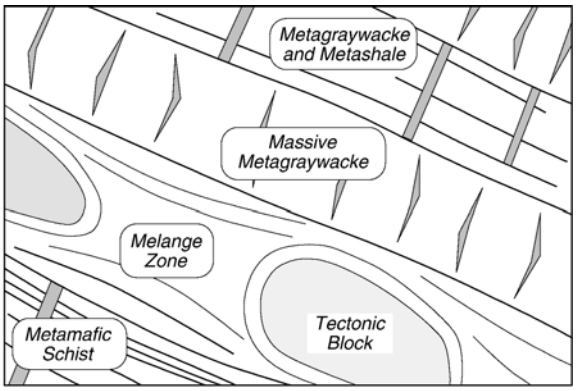

Fig. 9. Illustration of structural makeup of the Catalina Schist, consisting of adjacent domains of relatively coherent metasedimentary and metamafic sections with mélange zones thought to represent conduits for fluid mobility (see Bebout, 1991a,b, 1997). Fluid flow is believed to have occurred among highly chemically disparate lithologies (mélange, ultramafic, mafic, and sedimentary lithologies), probably enhancing the loss of trace elements from subducting sediments. Element mobility could be enhanced in mélange zones relative to more "coherent" mafic and sedimentary domains (Bebout and Barton, 2002; Breeding et al., 2004; Spandler et al., 2004; Bebout, in press).

Fig. 9 illustrates the lithologic juxtapositions typical of the Catalina Schist, that is, involving adjacent packages of metasedimentary rocks of varying types with metabasaltic domains and mélange zones. Fluids migrating through this section are expected to have moved largely along mélange zones, but in metasedimentary and metamafic sections, permeability is also enhanced by fracturing at various scales. In mélange zones, O and N isotope compositions show homogenization relative to compositions of nearby coherent metasedimentary rocks, indicative of larger fluxes of fluid along the mélange zones (Bebout, 1997). We suggest that devolatilization should be viewed as a larger-scale process involving interplay between deformation, permeability enhancement, fluid flow and focusing, and element mobility along more permeable zones such as mélange zones (Bebout and Barton, 1989, 1993, 2002; also see discussions by Barnicoat and Cartwright, 1995; Breeding et al., 2004; Spandler et al., 2004; King et al., 2004; see Graham et al., 1997, for review of interplay of deformation, reaction, lithology, and structure during metamorphic fluid flow). At the slab–mantle interface, individual "packets" of fluid might then derive from heterogeneous lithologies, mix, and interact with disparate rock types along their flow paths, in some cases driving devolatilization and element release. Such infiltration-driven reaction has also been proposed as a potentially important

mechanism during decarbonation of subducting carbonate-rich sediment sections (see Gorman et al., 2006). Kessel et al. (2005) similarly propose the flushing of sediment-rich zones between the subducting oceanic crust and overlying mantle wedge by large amounts of supercritical fluid generated in oceanic crust, resulting in effective removal of metasedimentary trace elements by these fluids.

Interestingly, in a number of equilibrium models taking into account various quasi-open system (Rayleigh-like) and open-system (infiltration-driven) devolatilization scenarios (e.g., Kerrick and Connolly, 2001; Gorman et al., 2006), significant loss of H_2O (and CO_2, for carbonate-bearing lithologies) is indicated in subducting seafloor sediments over the depth interval between that of subarc regions (generally >100 km) and that represented by the Catalina Schist (15–40 km). This depth interval of ~40–100 km roughly corresponds to the interval represented by the units of the Schistes Lustrés and by the UHP-metamorphosed seafloor section exposed at Lago di Cignana. Despite the heterogeneity of H_2O content among samples at any one grade in these rocks, and even though exhumation-related overprinting may be accompanied by some addition of H_2O, the data of Busigny et al. (2003) show a crude *decrease* in whole-rock H_2O concentration that could partly reflect the reactions identified in these models. This H_2O loss evidently was accomplished without significant loss of B, Li, Cs, Rb, and N, based on the whole-rock data in Busigny et al. (2003) and supported by the SIMS white-mica compositions obtained by Bebout et al. (2003, 2004; manuscript in preparation).

4.5. Effects of retrogradation in higher-grade units

Data for fine-grained white mica in the amphibolite-facies rocks (see data in Fig. 6B not included in the other plots demonstrating trends in mica compositions) highlight the need for analytical methods with high spatial resolution in studies of geochemical evolution of HP/UHP suites, which commonly show extensive overprinting due to exhumation history. Boron isotope data for whole-rocks and tourmaline (Nakano, 1998; Bebout and Nakamura, 2003) for higher-grade metasedimentary rocks also show the influence of retrogradation, particularly in the epidote–amphibolite and amphibolite units (see data for white micas in Figs. 2 and 6B). Sedimentary rocks metamorphosed at these and higher pressures are generally more retrogressed and geochemically overprinted than nearby metabasaltic lithologies (e.g., study of Trescolmen rocks by Zack et al., 2001, 2002), presumably because sediments are more pervasively deformed during exhumation, affording more extensive fluid–rock interactions (for discussion of overprinting at the UHP Lago di Cignana exposure, see van der Klauw et al., 1997; Reinecke, 1998).

4.6. Pegmatites and leucosomes in the amphibolite-facies unit (trace element behavior during partial melting)

Data for pegmatite/leucosome samples 6-2-23, 6-3-24 and 6-3-75 (Fig. 3) demonstrate the residence of B, Li, and the LILE in micas in the three samples. Each of these was derived by water-saturated partial melting of metasedimentary rocks at amphibolite-facies conditions (650–750 °C; 8–11 kbar; Sorensen and Barton, 1987). The data obtained in this study demonstrate inheritance of trace element signatures in leucosomes and pegmatites from their metasedimentary sources, with B, Li, Cs, Rb, Ba, and Sr all present in micas at concentrations similar to those in micas in their nearby hosts (Fig. 3). The partial melting in the amphibolite unit of the Catalina Schist occurred at temperatures anomalously high for depths near 40 km in thermally mature modern subduction zones (see Grove and Bebout, 1995; thermal models in Peacock, 1996). However, the data for these pegmatites and leucosomes provide an analogue to metasedimentary melting that may occur at deeper levels in relatively cool subduction zones, during subduction initiation or ridge-trench encounters, or during warmer subduction thought to have operated in the Archaen.

5. Conclusions

In this study, detailed SIMS analysis of white micas in the Catalina Schist metasedimentary suite, showing a wide range in peak metamorphic grade, confirms a model of loss of B and Cs, relative to the other LILE (K, Rb, Ba, Sr) and Li, as the result of devolatilization along increasingly higher-*T* prograde *P*–*T* paths (Bebout et al., 1999). With careful attention to avoiding micas with textures and major element chemistry indicating late-stage, exhumation-related growth (i.e., attempting to analyze only micas better representing recrystallization at peak conditions), it is possible to improve upon the whole-rock studies particularly of the higher-grade units (which show more abundant evidence for retrogradation). This study confirms the impressive ability of white mica to retain certain relatively fluid-mobile elements (e.g., B, Cs, N) to great depths in subduction zones (in this case, to ~40 km) when metamorphosed along relatively low-*T* prograde *P*–*T* paths considered to

be the norm in most modern subduction zones (cf. Busigny et al., 2003). In metasedimentary rocks subducted along warmer *P–T* paths, such as those experienced by the higher-grade Catalina Schist units (epidote–amphibolite and amphibolite; see Fig. 1), greater degrees of devolatilization and associated trace element loss would be expected. Warm paths such as these could be experienced in modern subduction zones only in early stages of initiation and involving subduction of extremely young oceanic lithosphere. Recent thermal models (van Keken et al., 2002) predict that, in the Cascadia margin (involving subduction of young, relatively warm oceanic lithosphere), subducting rocks at the top of the slab are encountering *P–T* conditions similar to those encountered during peak metamorphism of the epidote–blueschist unit in the Catalina Schist (~400 °C at 1 GPa; see Fig. 1), for which our data indicate significant losses of B and Cs related to enhanced devolatilization (see discussion by Bebout et al., 1999). Warmer subduction is thought to have dominated in the Archaen, pointing to dramatically different recycling behavior of these elements at subduction zones in the early Earth.

Acknowledgments

We acknowledge NERC support and funding from NSF grants (EAR92-06679 and EAR94-05625 to GEB; EAR94-05404 to AEB). We extend special thanks to John Craven, at the University of Edinburgh, for his help in acquiring the ion microprobe data during AEB's visit in 1994. We thank Adam Simon for his editorial handling of this manuscript, and the two reviewers for their helpful reviews. We also wish to thank Frank Kyte, at UCLA, for his help with the electron microprobe analyses.

References

Abbott, D., Lyle, M., 1984. Age of oceanic plates at subduction and volatile recycling. Geophys. Res. Lett. 11, 951–954.

Agard, P., Monie, P., Jolivet, L., Goffe, B., 2002. Exhumation of the Schistes Lustrés complex: in situ laser probe $^{40}Ar/^{39}Ar$ constraints and implications for the Western Alps. J. Metamorph. Geol. 20, 599–618.

Altheim, B.A., 1997. Low-grade metamorphism in the Catalina Schist: kinetic and tectonic implications. M.S. Thesis, Lehigh Univ., 80 pp.

Barnicoat, A.C., Cartwright, I., 1995. Focused fluid flow during subduction: oxygen isotope data from high-pressure ophiolites of the western Alps. Earth Planet. Sci. Lett. 132, 53–61.

Bebout, G.E., 1991a. Field-based evidence for devolatilization in subduction zones: implications for arc magmatism. Science 251, 413–416.

Bebout, G.E., 1991b. Geometry and mechanisms of fluid flow at 15 to 45 kilometer depths in an early Cretaceous accretionary complex. Geophys. Res. Lett. 18, 923–926.

Bebout, G.E., 1995. The impact of subduction-zone metamorphism on mantle–ocean chemical cycling. Chem. Geol. 126, 191–218.

Bebout, G.E., 1997. Nitrogen isotope tracers of high-temperature fluid–rock interactions: case study of the Catalina Schist, California. Earth Planet. Sci. Lett. 151, 77–90.

Bebout, G.E., in press. Chemical and isotopic cycling in subduction zones, Treat. Geochem., Elsevier.

Bebout, G.E., Barton, M.D., 1989. Fluid flow and metasomatism in a subduction zone hydrothermal system: Catalina Schist Terrane, California. Geology 17, 976–980.

Bebout, G.E., Fogel, M.L., 1992. Nitrogen-isotope compositions of metasedimentary rocks in the Catalina Schist, California: implications for metamorphic devolatilization history. Geochim. Cosmochim. Acta 56, 2139–2149.

Bebout, G.E., Barton, M.D., 1993. Metasomatism during subduction: products and possible paths in the Catalina Schist, California. Chem. Geol. 108, 61–92.

Bebout, G.E., Barton, M.D., 2002. Tectonic and metasomatic mixing in a high-temperature subduction-melange: insights into the geochemical evolution of the slab–mantle interface. Chem. Geol. 187, 79–106.

Bebout, G.E., Nakamura, E., 2003. Record in metamorphic tourmalines of subduction-zone devolatilization and boron cycling. Geology 31, 407–410.

Bebout, G.E., Ryan, J.G., Leeman, W.P., 1993. B–Be systematics in subduction-related metamorphic rocks: characterization of the subducted component. Geochim. Cosmochim. Acta 57, 2227–2237.

Bebout, A.E., Bebout, G.E., Graham, C.M., 1995. Ion microprobe evidence for the behavior of boron during devolatilization of metasedimentary rocks, Catalina Schist. Geol. Soc. Amer. Abstr. Progr. 26, 450.

Bebout, G.E., Ryan, J.G., Leeman, W.P., Bebout, A.E., 1999. Fractionation of trace elements during subduction-zone metamorphism: impact of convergent margin thermal evolution. Earth Planet. Sci. Lett. 171, 63–81.

Bebout, G., Agard, P., King, R., Nakamura, E., 2003. Geochemistry of devolatilization (and exhumation) in W. Alps HP and UHP metasedimentary suites. Geochim. Cosmochim. Acta 67, A36 [abstract for Goldschmidt Conference, Kurashiki, Japan].

Bebout, G.E., King, R., Agard, P., Kobayashi, K., Nakamura, E., 2004. Record of forearc devolatilization in the Schistes Lustrés HP–UHP metasedimentary unit Western Alps. Proc. Eleventh Water–Rock Symposium, Saratoga Springs.

Ben Othman, D., White, W.M., Patchett, J., 1989. The geochemistry of marine sediments, island arc magma genesis, and crust–mantle recycling. Earth Planet. Sci. Lett. 94, 1–21.

Benton, L.D., 1997. Origin and evolution of Serpentine Seamount Fluids, Mariana and Izu–Bonin Forearcs: implications for the recycling of subducted material, Ph.D. dissertation, Univ. Tulsa, 209 p.

Benton, L.D., Ryan, J.G., Tera, F., 2001. Boron isotope systematics of slab fluids as inferred from a serpentinite seamount, Mariana forearc. Earth Planet. Sci. Lett. 187, 273–282.

Blake, M.C., Jayko, A.S., McLaughlin, R.J., Underwood, M.B., 1987. Metamorphic and tectonic evolution of the Franciscan Complex, Northern California. In: Ernst, W.G. (Ed.), Metamorphism and Crustal Evolution of the Western United States. Rubey, vol. 7. Prentice-Hall, Englewood Cliffs, N. J, pp. 1035–1060.

Breeding, C.M., Ague, J.J., Bröcker, M., 2004. Fluid–metasedimentary rock interactions in subduction-zone mélange: implications for the chemical composition of arc magmas. Geology 32, 1041–1044.

Brunsmann, A., Franz, G., Erzinger, J., Landwehr, D., 2000. Zoisite- and clinozoisite-segregations in metabasites (Tauern Window,

Austria) as evidence for high-pressure fluid–rock interaction. J. Metamorph. Geol. 18, 1–21.
Brunsmann, A., Franz, G., Erzinger, J., 2001. REE mobilization during small-scale high-pressure fluid–rock interaction and zoisite/fluid partitioning of La to Eu. Geochim. Cosmochim. Acta 65, 559–570.
Busigny, V., Cartigny, P., Philippot, P., Ader, M., Javoy, M., 2003. Massive recycling of nitrogen and other fluid-mobile elements (K, Rb, Cs, H) in a cold slab environment: evidence from HP to UHP oceanic metasediments of the Schistes Lustrés nappe (western Alps, Europe). Earth Planet. Sci. Lett. 215, 27–42.
Catlos, E.J., Sorensen, S.S., 2003. Phengite-based chronology of K- and Ba-rich fluid flow in two paleosubduction zones. Science 299, 92–95.
Chan, L.H., Leeman, W.P., You, C.-F., 1999. Lithium isotopic composition of Central American volcanic arc lavas: implications for modification of subarc mantle by slab-derived fluids. Chem. Geol. 160, 255–280.
Domanik, K.J., Holloway, J.R., 1996. The stability and composition of phengitic muscovite and associated phases from 5.5–11 GPa; implications for deeply subducted sediments. Geochim. Cosmochim. Acta 60, 4133–4150.
Domanik, K.J., Hervig, R.L., Peacock, S.M., 1993. Beryllium and boron in subduction zone minerals: an ion microprobe study. Geochim. Cosmochim. Acta 57, 4997–5010.
Ernst, W.G., 1993. Metamorphism of Franciscan tectonostratigraphic assemblage, Pacheco Pass area, east-central Diablo Range, California Coast Ranges. Geol. Soc. Amer. Bull. 105, 618–636.
Fischer, T.P., Hilton, D.R., Zimmer, M.M., Shaw, A.M., Sharp, Z.D., Walker, J.A., 2002. Subduction and recycling of nitrogen along the Central American Margin. Science 297, 1154–1157.
Fryer, P., Mottl, M., Johnson, L., Haggerty, J., Phipps, S., Maekawa, H., 1995. Serpentine bodies in the forearcs of Western Pacific convergent margins: origin and associated fluids. In: Taylor, B., Natland, J. (Eds.), Active Margins and Marginal Basins of the Western Pacific. Amer. Geophys. Un. Geophys. Monogr., vol. 88, pp. 259–279.
Fryer, P., Wheat, C.G., Mottl, M.J., 1999. Mariana blueschist mud volcanism: implications for conditions within the subduction zone. Geology 27, 103–106.
George, R., Turner, S., Morris, J., Plank, T., Hawkesworth, C., Ryan, J., 2005. Pressure–temperature–time paths of sediment recycling beneath the Tonga–Kermadec arc. Earth Planet. Sci. Lett. 233, 195–211.
Gorman, P.J., Kerrick, D.M., Connolly, J.A.D., 2006. Modeling open system metamorphic decarbonation of subducting slabs. Geochem. Geophys. Geosyst. 7, Q04007. doi:10.1029/2005GC001125.
Graham, C.M., Skelton, A.D.L., Bickle, M.J., Cole, C., 1997. Lithological, structural and deformation controls on fluid flow during regional metamorphism. In: Holness, M.B. (Ed.), Deformation-Enhanced Fluid Transport in the Earth's Crust, vol. 8. Chapman and Hall, London, pp. 195–225.
Grove, M., Bebout, G.E., 1995. Cretaceous tectonic evolution of coastal southern California: insights from the Catalina Schist. Tectonics 14, 1290–1308.
Hart, S.R., Reid, M.R., 1991. Rb/Cs fractionation: a link between granulite metamorphism and the S-process. Geochim. Cosmochim. Acta 55, 2379–2382.
Hervig, R.L., 1985. Ion microprobe analysis of Li and B in silicate glasses (abstract). Eos, Trans. AGU 66, 401.
Hinton, R.W., 1990. Ion microprobe trace element analysis of silicates: measurement of multi-element glasses. Chem. Geol. 83, 11–25.
Hinton, R.W., 1999. NIST SRM 610, 611, and SRM 612, 613 multi-element glasses: constraints from element abundance ratios measured by microprobe techniques. Geostand. Lett. 23, 197–207.
Ishikawa, T., Nakamura, E., 1994. Origin of the slab component in arc lavas from across-arc variation of B and Pb isotopes. Nature 370, 205–208.
Ishikawa, T., Tera, F., 1997. Source, composition and distribution of the fluid in the Kurile mantle wedge: constraints from across-arc variations of B/Nb and B isotopes. Earth Planet. Sci. Lett. 152, 123–138.
Ishikawa, T., Tera, F., 1999. Two isotopically distinct fluid components involved in the Mariana arc: evidence from Nb/B ratios and B, Sr, Nd, and Pb isotope systematics. Geology 27, 83–86.
Ishikawa, T., Tera, F., Nakazawa, T., 2001. Boron isotope and trace element systematics of three volcanic zones in the Kamchatka arc. Geochim. Cosmochim. Acta 65, 4523–4537.
Johnson, M.C., Plank, T., 1999. Dehydration and melting experiments constrain the fate of subducted sediments. Geochem. Geophys. Geosyst. 1. doi:10.1029/1999GC000014.
Jones, A.P., Smith, J.V., 1984. Ion probe analyses of H, Li, B, F, and Ba in micas, with additional data for metamorphic amphibole, scapolite, and pyroxene. N. Jb. Miner. Mh. 228–240.
Kerrick, D.M., Connolly, J.A.D., 2001. Metamorphic devolatilization of subducted marine sediments and the transport of volatiles into the Earth's mantle. Nature 411, 293–296.
Kessel, R., Schmidt, M.W., Ulmer, P., Pettke, T., 2005. Trace element signature of subduction-zone fluids, melts and supercritical fluids at 120–180 km depths. Nature 437/29, 724–727.
King, R.L., Bebout, G.E., Kobayashi, K., Nakamura, E., van der Klauw, S.N.G.C., 2004. Ultrahigh-pressure metabasaltic garnets as probes into deep subduction zone chemical cycling. Geochem. Geophys. Geosyst. Q12J14. doi:10.1029/2004GC000746 Dec., 2004.
King, R.L., Bebout, G.E., Moriguti, T., Nakamura, E., 2006. Elemental mixing systematics and Sr–Nd isotope geochemistry of mélange formation: obstacles to identification of fluid sources to arc volcanics. Earth Planet. Sci. Lett. 246, 288–304.
Kirby, S., Engdahl, E.R., Denlinger, R., 1996. Intraslab earthquakes and arc volcanism: dual expressions of crustal and upper mantle metamorphism in subducting slabs. In: Bebout, G.E., Scholl, D.W., Kirby, S.H., Platt, J.P. (Eds.), Subduction: Top to Bottom. Amer. Geophys. Un. Geophys. Monogr., vol. 96, pp. 195–214.
Kovalenko, V.I., Hervig, R.L., Sheridan, M.F., 1988. Ion-microprobe analyses of trace elements in anorthoclase, hedenbergite, aenigmatite, quartz, apatite, and glass in pantellerite: evidence for high water contents in pantellerite melt. Am. Mineral. 73, 1038–1045.
Leeman, W.P., 1996. Boron and other fluid-mobile element systematics in volcanic arc lavas: implications for subduction processes. In: Bebout, G.E., Scholl, D.W., Kirby, S.H., Platt, J.P. (Eds.), Subduction: Top to Bottom. Amer. Geophys. Un. Geophys. Monogr., vol. 96, pp. 269–276.
Li, L., Bebout, G.E., 2005. Carbon and nitrogen geochemistry of sediments in the Central American convergent margin: insights regarding paleoproductivity and carbon and nitrogen subduction fluxes. J. Geophys. Res. 110, B11202. doi:10.1029/2004JB003276.
Manning, C.E., 2004. The chemistry of subduction-zone fluids. Earth Planet. Sci. Lett. 223, 1–16.
McDonough, W.F., Sun, S.-S., Ringwood, A.E., Jagoutz, E., Hofmann, A.W., 1992. Potassium, rubidium, and cesium in the Earth and Moon and the evolution of the mantle of the Earth. Geochim. Cosmochim. Acta 56, 1001–1012.
Melzer, S., Wünder, B., 2001a. K–Rb–Cs partitioning between phlogopite and fluid: experiments and consequences for the LILE signatures of island arc basalts. Lithos 59, 69–90.

Melzer, S., Wünder, B., 2001b. Island-arc basalt alkali ratios: constraints from phengite-fluid partitioning experiments. Geology 28, 583–586.

Mingram, B., Brauer, K., 2001. Ammonium concentration and nitrogen isotope composition in metasedimentary rocks from different tectonometamorphic units of the European Variscan Belt. Geochim. Cosmochim. Acta 65, 273–287.

Moran, A.E., 1993. The effect of metamorphism on the trace element composition of subducted oceanic crust and sediment. Ph.D. dissertation, Rice University.

Moran, A.E., Sisson, V.B., Leeman, W.P., 1992. Boron depletion during progressive metamorphism: implications for subduction processes. Earth Planet. Sci. Lett. 111, 331–349.

Moriguti, T., Nakamura, E., 1998. Across-arc variation of Li isotopes in lavas and implications for crust/mantle recycling at subduction zones. Earth Planet. Sci. Lett. 163, 167–174.

Moriguti, T., Shibata, T., Nakamura, E., 2004. Lithium, boron and lead isotope and trace element systematics of Quaternary basaltic volcanic rocks in northeastern Japan: mineralogical controls on slab-derived fluid composition. Chem. Geol. 212, 81–100.

Morris, J.D., Ryan, J.G., 2003. Subduction zone processes and implications for changing composition of the upper and lower mantle. Treat. Geochem., vol. 2, pp. 451–470.

Morris, J.D., Leeman, W.P., Tera, F., 1990. The subducted component in island arc lavas: constraints from Be isotopes and B–Be systematics. Nature 344, 31–36.

Mottl, M.J., Wheat, C.G., Fryer, P., Gharib, J., Martin, J.B., 2004. Chemistry of springs across the Mariana forearc shows progressive devolatilization of the subducting slab. Geochim. Cosmochim. Acta 68, 4915–4933.

Nakano, T., 1998. Boron isotope and trace element geochemistry of subduction-related metamorphic rocks: implications for the transportation of elements during metamorphism (Ph.D. dissertation). Misasa, Japan, Okayama University, 224 p.

Nakano, T., Nakamura, E., 2001. Boron isotope geochemistry of metasedimentary rocks and tourmalines in a subduction-zone metamorphic suite. Phys. Earth Planet. Inter. 127, 233–252.

Noll, P.D., Newsom, H.E., Leeman, W.P., Ryan, J.G., 1996. The role of hydrothermal fluids in the production of subduction zone magmas: evidence from siderophile and chalcophile trace elements and boron. Geochim. Cosmochim. Acta 60, 587–611.

Otamendi, J.E., de la Rosa, J.D., Patino Douce, A.E., Castro, A., 2002. Rayleigh fractionation of heavy rare earths and yttrium during metamorphic garnet growth. Geology 30, 159–162.

Pawley, A.R., 1994. The pressure and temperature stability limits of lawsonite: implications for H_2O recycling in subduction zones. Contrib. Mineral. Petrol. 118, 99–108.

Pawley, A.R., Holloway, J.R., 1993. Water sources for subduction zone volcanism; new experimental constraints. Science 260, 664–667.

Peacock, S.M., 1996. Thermal and petrologic structure of subduction zones. In: Bebout, G.E., Scholl, D.W., Kirby, S.H., Platt, J.P. (Eds.), Subduction: Top to Bottom. Amer. Geophys. Un. Geophys. Monogr., vol. 96, pp. 119–133.

Peacock, S.M., Hervig, R.L., 1999. Boron isotopic composition of subduction-zone metamorphic rocks. Chem. Geol. 160, 281–290.

Phinney, D., Whitehead, B., Anderson, D., 1979. Li, Be, and B in minerals of a refractory-rich Allende inclusion. Proc. Lunar Planet. Sci. Conf. 10, 885–905.

Plank, T., Langmuir, C.H., 1993. Tracing trace elements from sediment input to volcanic output at subduction zones. Nature 362, 739–743.

Plank, T., Langmuir, C., 1998. The chemical composition of subducting sediment and its consequences for the crust and mantle. Chem. Geol. 145, 325–394.

Rea, D.K., Ruff, L.J., 1996. Composition and mass flux of sedimentary materials entering the World's subduction zones: implications for global sediment budgets, great earthquakes, and volcanism. Earth Planet. Sci. Lett. 140, 1–12.

Reinecke, T., 1998. Prograde high- to ultrahigh-pressure metamorphism and exhumation of oceanic sediments at Lago di Cignana, Zermatt–Saas Zone, western Alps. Lithos 42, 147–189.

Rosner, M., Erzinger, J., Franz, G., Trumbull, R.B., 2003. Slab-derived boron isotope signatures in arc volcanic rocks from the Central Andes and evidence for boron isotope fractionation during progressive slab dehydration. Geochem. Geophys. Geosyst. 4. doi:10.1029/2002GC000438.

Ryan, J.G., Morris, J.D., Tera, F., Leeman, W.P., Tsvetkov, A., 1995. Cross-arc geochemical variations in the Kurile island arc as a function of slab depth. Science 270, 625–628.

Ryan, J., Morris, J., Bebout, G., Leeman, B., Tera, F., 1996. Describing chemical fluxes in subduction zones: insights from "depth-profiling" studies of arc and forearc rocks. In: Bebout, G.E., Scholl, D.W., Kirby, S.H., Platt, J.P. (Eds.), Subduction: Top to Bottom. Amer. Geophys. Un. Geophys. Monogr., vol. 96, pp. 263–268.

Sadofsky, S.J., Bebout, G.E., 2001. Paleohydrogeology at 5–50 kilometer depths of accretionary prisms: the Franciscan Complex, California. Geophys. Res. Lett. 28, 2309–2312.

Sadofsky, S.J., Bebout, G.E., 2003. Record of forearc devolatilization in low-*T*, high-*P*/*T* metasedimentary suites: significance for models of convergent margin chemical cycling. Geochem. Geophys. Geosyst. 4.

Sadofsky, S.J., Bebout, G.E., 2004. Field and isotopic evidence for fluid mobility in the Franciscan Complex: forearc paleohydrogeology at 5–50 kilometer depths. Int. Geol. Rev. 46, 1053–1088.

Sedlock, R.L., 1988. Metamorphic petrology of a high pressure, low temperature subduction complex in West-Central Baja California, Mexico. J. Metamorph. Geol. 6, 205–233.

Shibata, T., Nakamura, E., 1997. Across-arc variations of isotope and trace element compositions from Quaternary basaltic volcanic rocks in northeastern Japan: implications for interaction between subducted slab and mantle wedge. J. Geophys. Res. 102, 8051–8064.

Shimizu, N., Semet, M.P., Allègre, C.J., 1978. Geochemical applications of quantitative ion-microprobe analysis. Geochim. Cosmochim. Acta 42, 1321–1334.

Smith, H.J., Leeman, W.P., Davidson, J., Spivack, A.J., 1997. The B isotopic composition of arc lavas from Martinique, Lesser Antilles. Earth Planet. Sci. Lett. 146, 303–314.

Sorensen, S.S., 1984. Petrology of basement rocks of the California Continental Borderland and the Los Angeles Basin. Ph. D. Thesis, Univ. Calif., Los Angeles, Ca.

Sorensen, S.S., 1986. Petrologic and geochemical comparison of the blueschist and greenschist units of the Catalina Schist terrane, southern California. Geol. Soc. Amer. Mem. 164, 59–75.

Sorensen, S.S., Barton, M.D., 1987. Metasomatism and partial melting in a subduction complex, Catalina Schist, southern California. Geology 15, 115–118.

Sorensen, S.S., Grossman, J.N., Perfit, M.R., 1997. Phengite-hosted LILE-enrichment in eclogite and related rocks: implications for fluid-mediated mass transfer in subduction zones and arc magma genesis. J. Petrol. 38, 3–34.

Spandler, C., Hermann, J., Arculus, R., Mavrogenes, J., 2004. Geochemical heterogeneity and element mobility in deeply

subducted oceanic crust; insights from high-pressure mafic rocks from New Caledonia. Chem. Geol. 206, 21–42.

Staudigel, H., King, S.D., 1992. Ultrafast subduction: the key to slab recycling efficiency and mantle differentiation? Earth Planet Sci. Lett. 109, 517–530.

Straub, S.M., Layne, G.D., 2003. Decoupling of fluids and fluid-mobile elements during shallow subduction: evidence from halogen-rich andesite melt inclusions from the Izu arc volcanic front. Geochem. Geophys. Geosyst. 4. doi:10.1029/2002GC000349.

Syracuse, E.M., Abers, G.A., 2006. Global compilation of variations in slab depth beneath arc volcanoes and implications. Geochem. Geophys. Geosyst. 7, Q05017. doi:10.1029/2005GC001045.

Tomascak, P.B., Ryan, J.R., Defant, M.J., 2000. Lithium isotope evidence for light element decoupling in the Panama subarc mantle. Geology 28, 507–510.

Tomascak, P.B., Widom, E., Benton, L.D., Goldstein, S.L., Ryan, J.G., 2002. The control of lithium budgets in island arcs. Earth Planet. Sci. Lett. 196, 227–238.

Usui, T., Nakamura, E., Helmstaedt, H., 2006. Petrology and geochemistry of eclogite xenoliths from the Colorado Plateau: implications for the evolution of subducted oceanic crust. J. Petrol. 47, 929–964.

van der Klauw, S.N.G.C., Reinecke, T., Stockhert, B., 1997. Exhumation of ultrahigh-pressure metamorphic oceanic crust from Lago di Cignana, Piemontese zone, western Alps: the structural record in metabasites. Lithos 41, 79–102.

van Keken, P.E., Kiefer, B., Peacock, S.M., 2002. High-resolution models of subduction zones: implications for mineral dehydration reactions and the transport of water into the deep mantle. Geochem. Geophys. Geosyst. 3, 1056. doi:10.1029/2001GC000256.

von Huene, R., Scholl, D.W., 1991. Observations at convergent margins concerning sediment subduction, subduction erosion, and the growth of continental crust. Rev. Geophys. 29, 279–316.

You, C.F., Castillo, P.R., Gieskes, J.M., Chan, L.H., Spivack, A.J., 1996. Trace element behavior in hydrothermal experiments: implications for fluid processes at shallow depths in subduction zones. Earth Planet. Sci. Lett. 140, 41–52.

You, C.F., Spivack, A.J., Gieskes, J.M., Rosenbauer, R., Bischoff, J.L., 1995. Experimental study of boron geochemistry: implications for fluid processes in subduction zones. Geochim. Cosmochim. Acta 59, 2435–2442.

Zack, T., Rivers, T., Foley, S.F., 2001. Cs–Rb–Ba systematics in phengite and amphibole: an assessment of fluid mobility at 2.0 GPa in eclogites from Trescolmen, Central Alps. Contrib. Mineral. Petrol. 140, 651–669.

Zack, T., Foley, S.F., Rivers, T., 2002. Equilibrium and disequilibrium trace element partitioning in hydrous eclogites (Trescolmen, Central Alps). J. Petrol. 43, 1947–1974.

Zack, T., Tomascak, P.B., Rudnick, R.L., Dalpe, C., McDonough, W.F., 2003. Extremely light Li in orogenic eclogites: the role of isotope fractionation during dehydration in subducted oceanic crust. Earth Planet. Sci. Lett. 208, 279–290.